"Green", innovative, versatile and efficient carbon materials from polyphenolic plant extracts

Alain Celzard, Vanessa Fierro

“Green”, innovative, versatile and efficient carbon materials from polyphenolic plant extracts

Alain Celzard[1] and Vanessa Fierro[2]

Institut Jean Lamour, UMR CNRS – Université de Lorraine n°7198. ENSTIB, 27 rue Philippe Séguin, BP 21042, 88051 Epinal cedex 9, France

[1]Corresponding author. Tel: + 33 372 74 96 14. Fax: + 33 372 74 96 38. E-mail address : Alain.Celzard@univ-lorraine.fr (A. Celzard)

[2]Corresponding author. Tel: + 33 372 74 96 77. Fax: + 33 372 74 96 38. E-mail address : Vanessa.Fierro@univ-lorraine.fr (V. Fierro)

Abstract

Tannins are polyphenolic molecules of great industrial interest, not only for themselves but also as bio-based precursors for multiple carbonaceous materials with extremely diverse structures, textures and potential applications. In recent years, extensive work has been devoted to these new, predominantly porous carbons, and to their properties. It was therefore time to collect the main results in this invited review, whose objective is to show how a single, inexpensive, non-toxic and commercially available renewable resource can lead to such a wide range of different carbons. Cellular carbons, ordered or disordered mesoporous carbons, carbon gels and vitreous carbons, among others, are presented herein through their textures, morphologies and applications. We show that some of these tannin-derived materials are truly model materials, in the sense of excellent control of their structure. Therefore, they could be successfully used to verify the applicability of certain laws of physics to these carbons, or to observe their limits, for the first time. We end this article with a quick overview of the studies still underway in this area.

Keywords: Tannins; Porous carbons; Functional carbons; Cellular carbons; Mesoporous carbons; Vitreous carbon

1. Introduction

While the various “nano” forms of carbon have been so popular in recent years and are being more than ever actively investigated worldwide, which is fully justified with respect to their amazing properties [1–3], one should not forget the potential of bio-based carbons for the extraordinary range of technological solutions they can offer. Especially, the vast majority of them are porous carbons, whose economic and environmental importance is considerable. For instance, porous carbons are found in many industrial processes or are still the subject of very active research in the following domains, amongst others: heat management (heat transfer [4], thermal insulation [5], and solar energy storage [6–11]); gas storage [12,13], compression [14,15], detection and separation [16–20]; storage and conversion of electrochemical energy (supercapacitors [21,22], batteries [23,24] and fuel cells [25,26]); catalysis [27,28], photocatalysis [29,30] and electrocatalysis [31]; pollutants removal in gas [32–34] or liquid [32,35–40] phase; protection against electromagnetic waves [41–44].

Given the major role played by porous materials, the search for natural, renewable, inexpensive but also effective precursors appears to be a meaningful quest. The diversity of possible compositions and the different porosity scales that are involved allow considering bio-based raw materials for all the aforementioned applications.

The great originality of the works presented in this review, though not completely exhaustive, is that an exceptionally broad range of carbon materials can be synthesised and optimised for an exceptionally vast spectrum of applications, based on a single resource extracted from plants: tannins. This phenolic material combines in a unique way a number of exceptional advantages, among them cheapness, commercial availability, renewable character, absence of toxicity but high reactivity, high carbon yield, as well as, last but not

least, an excellent reproducibility, which is a very rare feature as far as a bioresource is concerned. We show below how such precursor can lead to bio-resins whose porous structure and chemistry can be controlled before pyrolysis to an extent never proposed before, thus directly influencing the architecture, the nanotexture and the chemistry of the resultant carbons.

This review aims to summarise a bit more than 10 years of work from our research team at Institut Jean Lamour. The sum of these works has earned us to be rewarded with the Charles E. Pettinos Award, established and supported by the Charles E. and Joy C. Pettinos Foundation and administered and presented by the American Carbon Society every three years. The purpose of this award, offered to us in July 2019 during the Carbon'19 conference held in Lexington, Kentucky (USA), is to recognise recent outstanding research accomplishments of an individual or group in the science and/or technology of carbon materials, and to commemorate Charles E. Pettinos for his contributions to the graphite industry.

In the following, various carbonaceous materials designed for various applications are thus described. But we also demonstrate that carbons prepared with highly controlled structures and compositions can become model materials for testing and/or improving various theories developed by physicists and physico-chemists (e.g. in condensed matter physics, mechanics, electrodynamics, adsorption, see below), whether for the in-depth characterisation of (nano)porosity or for describing the properties of porous solids. Therefore, beyond the only technological - yet very important aspects - related to porous carbons, these studies also allowed conjugating in a unique way resources extracted from the living, carbon science, and high-level academic research in physics.

The present paper summarises the articles already published on the topic of new carbons derived from plant extracts, especially condensed tannins, by giving an overview of the

concepts and presenting the key results without ever going too much into detail. The interested reader can indeed refer to the numerous references given throughout the text. We also took the opportunity to introduce original results as well as some work in progress, which will be the subject of forthcoming publications.

2. Carbon derived from condensed tannins

2.1 A short introduction to polyphenols

"Polyphenols" is a generic term referring to a very broad family of most of the time natural molecules. They have the common feature of being based on a small aromatic group, "phenol", which is a toxic and carcinogenic molecule when considered alone. However, in the form of polyphenols, the corresponding compounds are extremely important in nutrition, medicine and cosmetics as they can be either protective against various things (photo-protective, vasoprotective, neuroprotective, etc.) or act as "anti-something" (anti-oxidant, anti-mutagenic, anti-cancer, anti-fungal, anti-bacterial, anti-diabetic, etc.) [45–49]. Polyphenols are indeed found in almost every part of plants: roots, leaves, flowers, stems and fruits, where their main purpose is to protect the plants against UV-light, herbivores, or bacterial and fungal infections [50–53].

Polyphenols are usually divided into four main groups: phenolic acids, flavonoids, stilbenes and lignans. Out of them, tannins are of special interest as precursors of carbon materials, and are indeed the object of the present article. However, tannins is a somewhat ambiguous terminology, since many kinds of natural molecules can be found under such very general name [54]. For instance, "condensed tannins" belong to the flavonoid group and in particular to the flavanols subgroup, where monomers such as catechin, among others, are

building units of oligomers and larger natural polymers. In contrast, hydrolysable tannins belong to the family of phenolic acids. More details about the broad tannin family can be found elsewhere [55,56] and typical chemical structures of a few examples are presented in Figure 1.

(a)

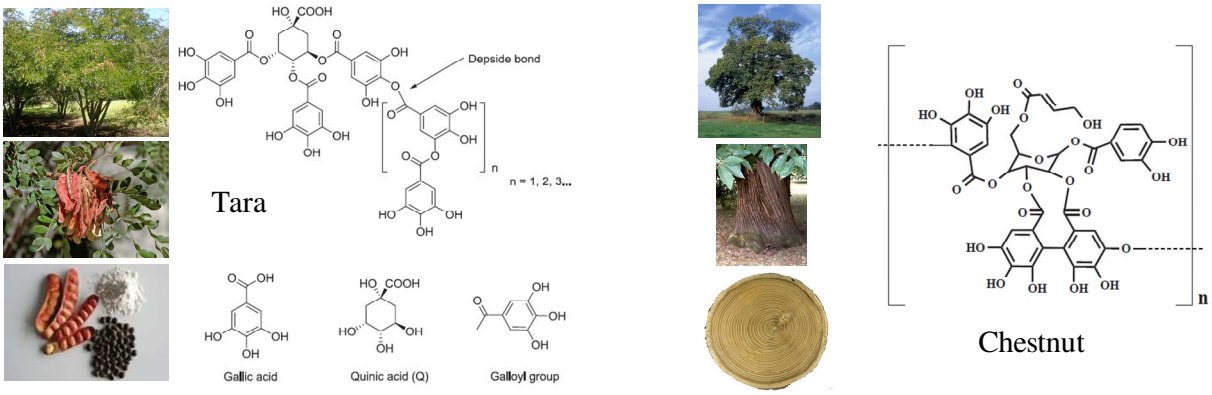

(b)

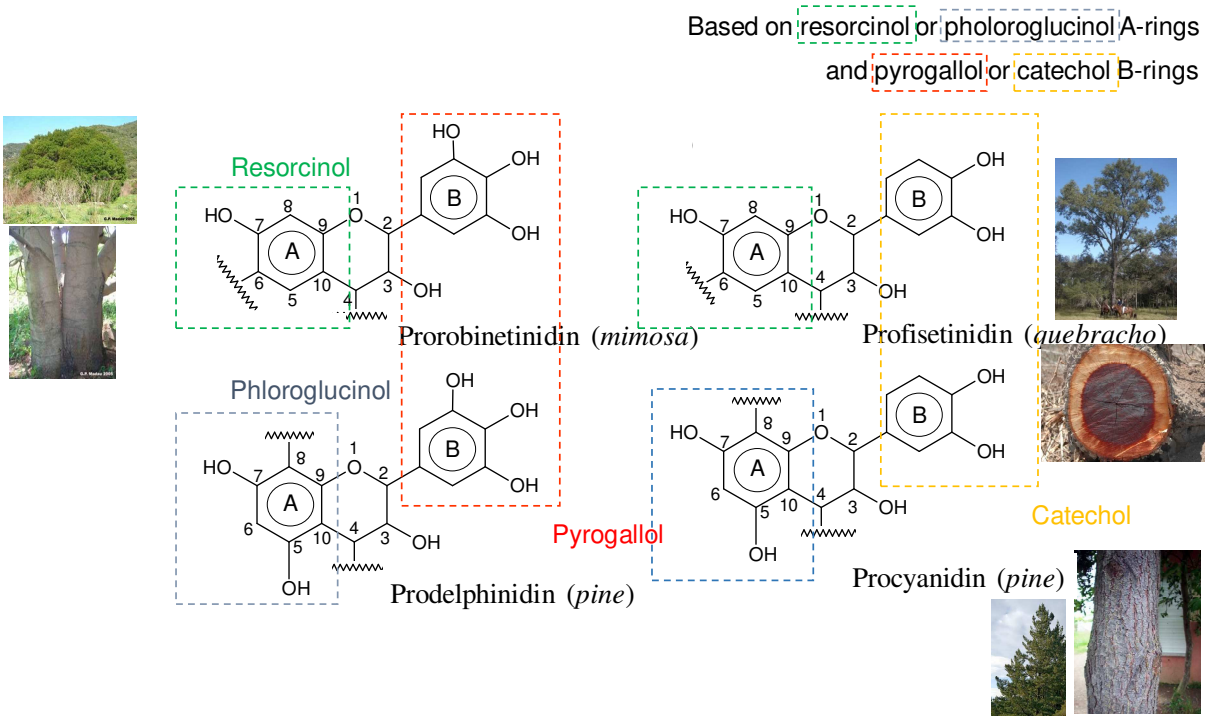

Figure 1. Typical chemical structure of: (a) two examples of hydrolysable tannins, from tara (*Caesalpinia spinosa*, left) and chestnut (*Castanea sativa*, right), and (b) four examples of

condensed tannins, from mimosa (*Acacia mearnsii*, top left), quebracho (*Shinopsis balansae*, top right), and pine (*Pinus radiata*, bottom). (Reprinted from [57] and [58] with permission from Elsevier, and from [56] with permission from Springer).

Tannins share the advantage of being natural and hence renewable, non-toxic though reactive, cheap, and soluble in water and protic solvents. Importantly, most of tannins are also commercially available in reproducible quality, making them serious competitors of synthetic, hazardous, phenolic molecules. Although still rather poorly known, these bioresources have a surprisingly high number of applications [59]. However, from one kind of tannin to another, the situations are contrasted. Thus, hydrolysable tannins present a limited interest as far as the preparation of carbon materials is concerned. They indeed react rather slowly with aldehydes, the presence of which is generally necessary for crosslinking them, but even after reaction the molecular weights are not that high, and the level of phenol substitution is low. As a result, and even if carbon materials can be prepared and have been reported [58,60,61], the carbon yield is poor. Therefore, these precursors will not be discussed any longer in the rest of this paper. In contrast, condensed tannins are easily crosslinked with most common aldehydes and can produce high-quality phenolic-furanic resins in the presence of furfuryl alcohol [62,63]. They can even auto-condense in the presence of some catalysts [64,65]. Whatever the way they are produced, and whether they are furanic or not, these thermoset resins based on condensed tannins are excellent precursors of carbon materials.

2.2 Generalities about carbon derived from condensed tannins

Because of the highly aromatic nature of such phenolic precursors, once crosslinked, resins based on tannins maintain their original structure and morphology when submitted to pyrolysis, present an excellent carbon yield (about 47 ± 3%), and lead to non-graphitisable (glassy) carbon in the absence of any graphitisation catalyst.

Its main physical characteristics are the following. The skeletal density is high for a glassy carbon, 1.98 ± 0.02 g/cm^3, a value systematically recovered for multiple tannin-based carbons, whatever their morphology (powders, rigid foams, aerogels or solid blocks) [66–72]. The electrical and thermal conductivities are 1055 S/m [73] and 3.8 W/m/K [74], respectively; these values were indirectly determined from a number of materials of different porosities. Another feature is that, during pyrolysis, the weight loss is very well compensated by the volume shrinkage, so that the bulk density before and after pyrolysis is unchanged [75]. Such behaviour, again, has been observed with a number of formulations based on condensed tannins (see for instance Figure 2(a)). Therefore, since the skeletal density of the resultant carbon is higher than that of the resin precursor, the porosity increases during carbonisation [68].

In the absence of graphitisation catalyst, carbon materials derived from tannins remain in the carbonisation regime (as opposed to the graphitisation regime), no matter high the heat-treatment temperature. This is proved by the continuous increase of the D/G band intensity ratio seen in Raman spectra (Figure 2(b)) whereas the FWHM of these bands decreases at the same time. In contrast, the materials enter the graphitisation regime since 900°C as soon as Fe is present and, even better, Ni. In this regime, the Raman spectra indeed show an opposite trend, with a sharp decrease of the D/G ratio, accompanied by a narrowing of these bands and a marked structuration of the second order (between 2500 et 3000 cm^{-1}, see again Figure 2(b)).

Tannin-based glassy carbon has a coefficient of thermal expansion of 3.53×10^{-6} K^{-1} up to 300°C, which value is very typical of an ordinary glassy carbon made of furfuryl alcohol [76]. However, a structural relaxation may be clearly observed during the first heating cycle after synthesis (see Figure 2(c)), which tends to disappear during the following heating cycles and whose amplitude depends on the heating rate used during the pyrolysis of the tannin-based

resin [77]. It could be added that the Young's modulus of bulk tannin-based carbon prepared at 900°C is close to 9.5 GPa, as determined by nanoindentation with a spherical tip. The details of such measurements will be the object of a forthcoming publication.

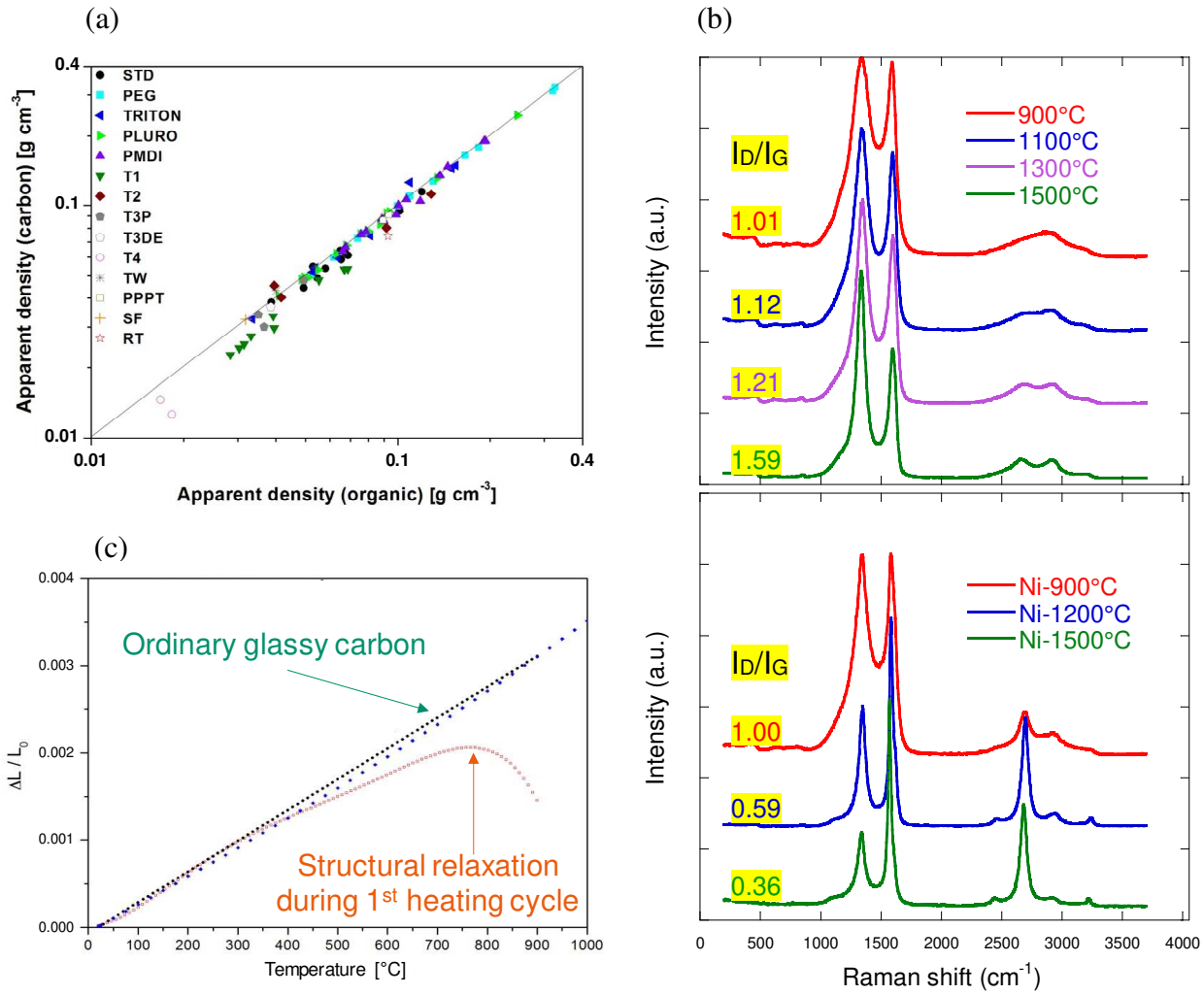

Figure 2. A few characteristics of tannin-based carbon: (a) unchanged bulk density of tannin-based thermoset resins during pyrolysis at 900°C; (b) Raman spectra showing the non-graphitisable (top) or graphitisable character (bottom) of tannin-based materials, whether Ni is absent or present in the formulation, respectively; (c) Thermal expansion of tannin-derived glassy carbon during its first heating to 900°C after synthesis (after [77], and from [75] with permission from Elsevier).

Tannin is mostly obtained by extraction of wood chips or barks with hot aqueous solutions, which are subsequently spray-dried [78]. As a result, hollow particles are obtained, which maintain their structure if such tannin powder is directly carbonised instead of being used for producing resins as carbon precursors. The result is shown in Figure 3(a). This carbon material is characterised by very narrow pores, as suggested by its N_2 and CO_2 isotherms measured at -196°C and 0°C, respectively, and the corresponding pore-size distribution obtained by application of the NLDFT method [79] to both isotherms at the same time (Figure 3(b)). Whereas the classical BET method suggests a negligibly low surface area, the NLDFT leads to a value of 770 m^2/g, with a micropore volume of 0.20 cm^3/g and an average micropore width of 0.55 nm.

(a)

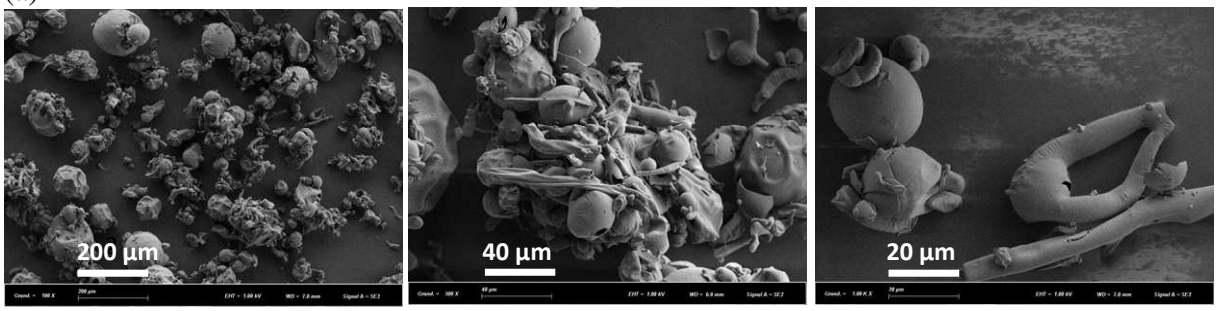

(b)

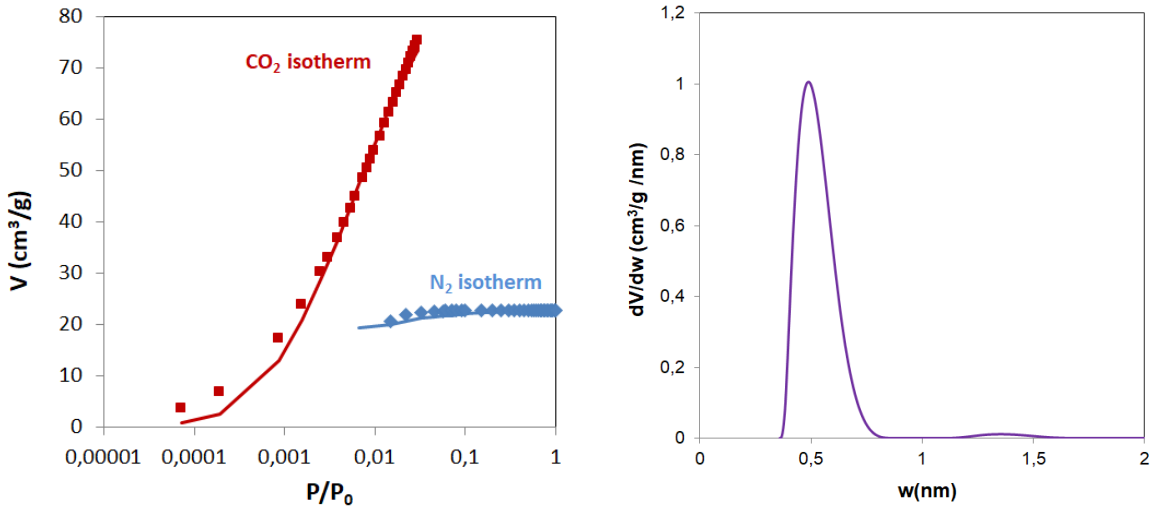

Figure 3. Particles of commercial condensed tannins (extracted from mimosa barks and supplied under the name FINTAN OP by the company Silva (Italy)) after direct carbonisation at 900°C: (a) SEM pictures at different magnifications, and (b) pore texture analysis through N_2 (-196°C) and CO_2 (0°C) isotherms, fitted by the NLDFT model (left), and corresponding pore-size distribution (right).

Table 1 shows the elemental composition of commercial condensed tannin particles (from *mimosa*) before and after direct carbonisation at 900°C. It can be seen that a significant amount of oxygen is still present, partly due to furanic structures having survived pyrolysis in the carbon structure [80,81]. Such significant amount of residual heteroelements, associated with the narrow, pre-existing porosity of carbonised tannin particles, explains how easy tannin-based carbon can be activated. Figure 4 shows for instance the effect on burn-off of steam and CO_2 activation at 800°C and 900°C, respectively (Figure 4(a)), BET area (Figure 4(b)), and micro and mesopore volumes (Figure 4(c)). Figure S1 of the Supplementary Information also unambiguously shows the very different effects of steam and CO_2 activation on the nitrogen adsorption isotherms and corresponding pore-size distributions: CO_2 produces more micropores and much less mesopores than steam activation.

Table 1. Elemental composition of mimosa tannin before and either after direct pyrolysis at 900°C, or after hydrothermal carbonisation (HTC: 180°C, 1h) and subsequent pyrolysis at 900°C.

Element (wt. %)	Before pyrolysis	After direct pyrolysis at 900°C	After HTC and then pyrolysis at 900°C
C	53.80	90.37	88.32
H	5.40	0.82	0.94
O	40.10	8.25	10.07
N	0.60	0.56	0.65

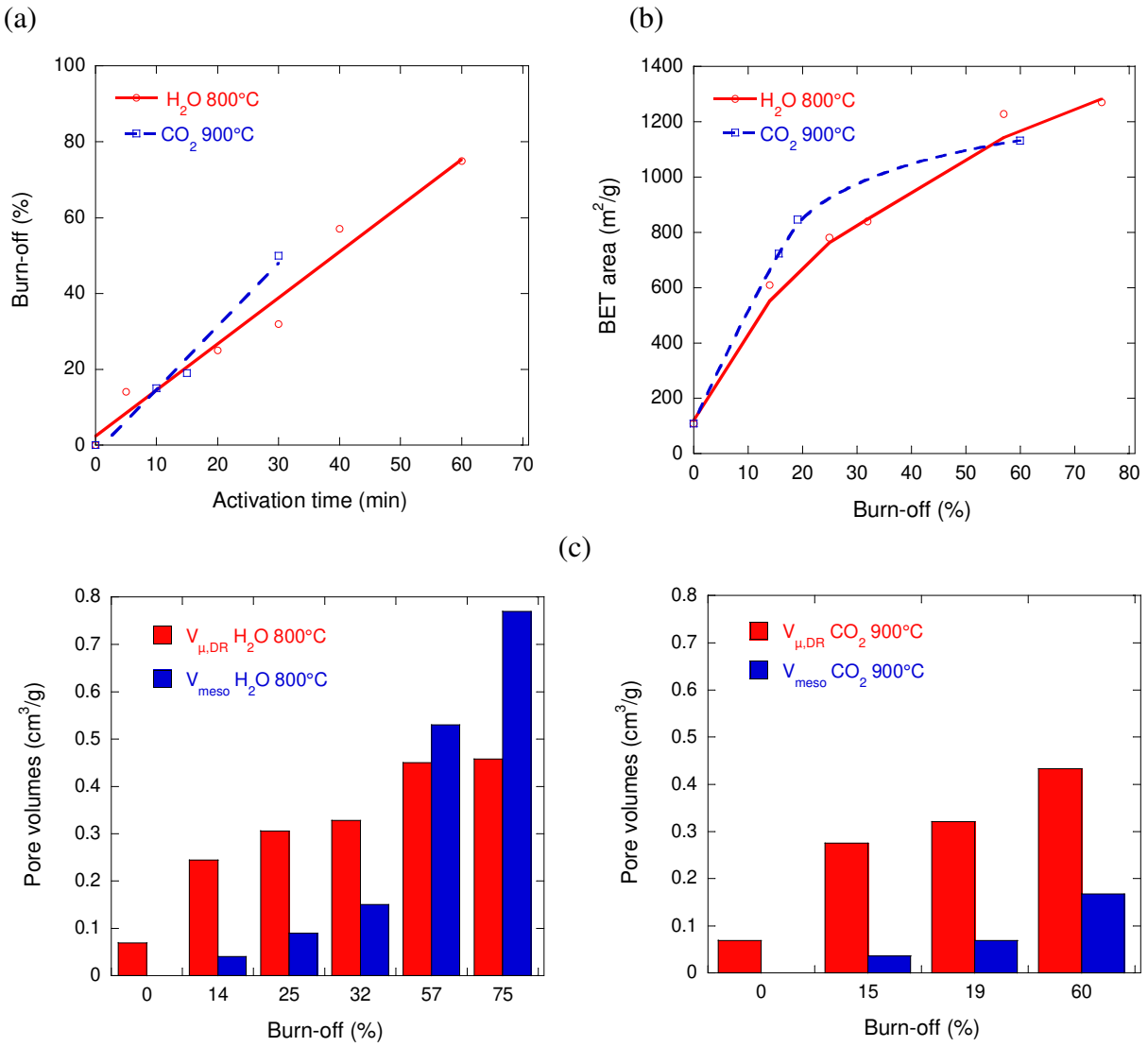

Figure 4. Effect of steam and CO_2 activation at 800°C and 900°C, respectively, on: (a) burn-off; (b) BET area; and (c) micro ($V_{\mu DR}$) and mesopore (V_{meso}) volumes [79].

In the following, recent achievements as well as presently ongoing studies are briefly described to illustrate the versatility of tannins for producing an extremely broad range of functional carbon materials. For that purpose, resins or solutions based on tannin are generally produced, which once foamed, gelled, bulk-crosslinked, mesostructured, or deposited on templates in hydrothermal conditions, amongst other methods, lead to all kinds of carbon structures, from the nano to the macroscale, graphitised or not, with very different but controlled porosities, and hence with a number of technological applications.

3. Cellular carbons

3.1 Vitreous carbon foams

3.1.1 *Preparation of model vitreous carbon foams*

Tannin-based foams can be prepared by multiple ways, including physical, chemical, or mixed foaming. The many experimental parameters with which it is possible to play (temperature, nature and amount of plasticisers, surfactants and other additives, amongst others) allow obtaining adjustable bulk density, cell size and connectivity of the resultant rigid or semi-elastic foams. About 70 different carbon foams could thus be prepared, based on different types of formulations, using different amounts of blowing agents and different foaming methods, a selection of which is presented in Figure 5(a). Cellular foams, i.e., having cell walls, and reticulated foams, i.e., only based on struts, were obtained and investigated by micro-computed X-ray tomography (µ-CT) and SEM. The application of stereology principles to SEM pictures, i.e., the three-dimensional interpretation of two-dimensional cross-sections of materials based on several techniques and related equations, confirmed the relevance of electron microscopy, since the same values of cell sizes could be successfully derived, as shown in Figure 5(b). The use of SEM is thus recommended, since much easier, faster and with higher resolution than µ-CT (here limited to 5 µm), as long as no more detailed structural information is required.

Finally, all these materials allowed obtaining Figure 5(c), of key importance for modelling studies. In this plot, all fits are application of power laws that relate bulk density to average cell size, and correspond to different kinds of formulations. Figure 5(c) shows above all that it is possible to find several independent series of carbon foams having very different densities (and thus very different porosities) at one constant given average cell size, on the one hand, and to

find several independent series of carbon foams having very different average cell sizes at one constant given bulk density, on the other hand. Such series of materials are obtained by drawing horizontal and vertical lines, respectively, across the plot. XRD and Raman studies have shown that the carbon skeleton has the same structure and nanotexture for the whole set of samples, and elemental analysis proved that the chemical composition was also the same (on average, in wt.%: C 90.7; H 1.1; O 6.9; N 0.6; S 0.7). Therefore it has been possible, for the first time, to decorrelate porosity and cell size while in the case of usual foams, larger porosities always correspond to larger cells. In the present case, through the selection of sample families from Figure 5(c), it has been possible, for instance, to find carbon foams with high porosity but very small cells or, on the contrary, to find carbon foams with very large cells but much lower porosity.

(a)

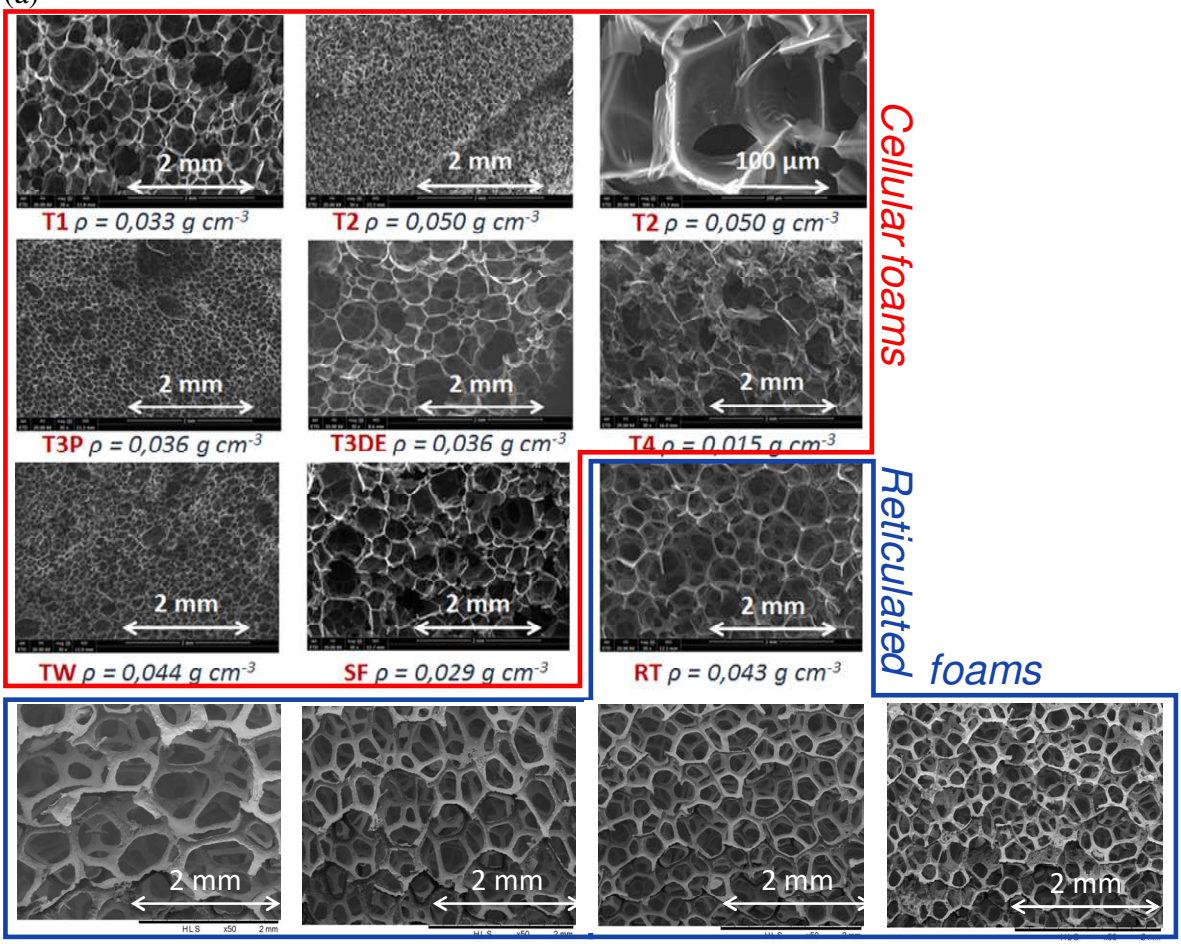

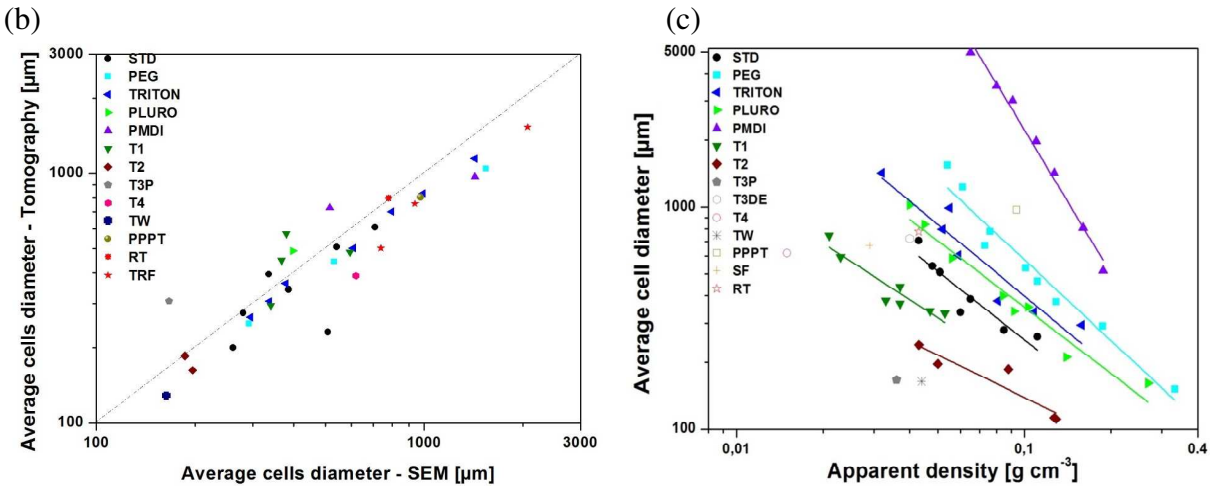

Figure 5. Cellular and reticulated carbon foams used as model materials in which porosity and cell size could be decorrelated: (a) SEM pictures of representative examples; (b) Excellent agreement between tomography and SEM studies; (c) Plot showing the possibility of finding series of samples having either different cell sizes at one given density (by drawing vertical lines across the plot), or having different densities (i.e., porosities) at one given cell size (by drawing horizontal lines across the plot). The solid lines are fits to the power law relating the cell size (D) to the bulk density of the foams (ρ): $D \propto \rho^{-x/y}$, where x and y are exponents from two other power laws involving the mass of boiling agent in the formulation (m_{ba}): $m_{ba} \propto \rho^{-x} \propto D^{-y}$ (Adapted from [75] with permission from Elsevier.

3.1.2 *Physical properties of model vitreous carbon foams*

Such model materials thus allowed exceptionally precise investigations of physical properties, which are briefly summarised below. For instance, it could be unambiguously shown that both Young's modulus and compressive strength are independent from cell size (see Figure S2(a)) [82]. In contrast, concerning the acoustic properties, the air permeability does not depend on total porosity but on cell size, and cellular and reticulated foams follow different behaviours (see Figure S2(b)) [83]. An optimum in air permeability was clearly identified, at which the absorption coefficient of sound (averaged on the frequency range of

800-6300 Hz) is maximum, and both reticulated and cellular foams converge towards the same optimum value (see Figure S2(c)). Finally, the concept of double porosity could also be successfully applied to cellular carbon foams, which consists in drilling holes inside the porous materials to produce the appearance of sound absorption peaks (see Figure S2(d)) at a frequency which can be tuned, depending on the diameter of the hole [84].

As for thermal properties, the studies revealed the significant effect of the porosity and the comparatively modest impact of cell size on thermal conductivity at room temperature [85]. In the infrared range, vitreous carbon foams behave as grey materials, i.e., have a roughly constant absorbance on a broad range of wavelengths, whereas their emissivity increases with temperature. Both quantities decrease when the cell size increases [86].

Regarding the electromagnetic properties, the independence of permittivity and electrical conductivity from cell size was evidenced, only the contribution of density (and hence of porosity) being significant (see Figures S3(a) and S3(b)) [87]. The changes of electrical conductivity with temperature could be very well fitted by Mott's law (see Figure S3(c)), which is the signature of variable-range hopping conduction mechanism in disordered, non-crystalline materials. This law involves the dimensionality of the system considered, and Table 2 clearly shows that this quantity increases with the density of the carbon foams. This finding is related to the fact that the higher is the density, the thicker are the cell walls, and hence the behaviour is progressively shifted from an almost 2D to 3D [88]. Finally, the electromagnetic properties investigated in the high-frequency range revealed very different behaviours of cellular and reticulated vitreous carbon foams. The latter exhibit a transmission peak, which has been attributed to a waveguide effect. Such effect was supported by considering cells as rectangular waveguides and calculating both the cut-off frequency of the fundamental (TE_{10}) mode (i.e., the lowest frequency for which this mode propagates in the

waveguide) and the maximum transmission frequency. Figure S3(d) shows the excellent agreement between such measured and calculated frequencies, thus explaining that carbon foams behave as band-pass filters.

Table 2. Parameters of Mott's law: $\sigma_{dc} = \sigma_0 \exp [- (T_M / T)^{1/n}]$, where $n = 1 + d_m$, fitted to the data of Figure S3(c); d_m is the dimensionality of the system in which variable-range hopping takes place.

Bulk density (g/cm^3)	Ln [σ_0 (S/m)]	T_M (K)	d_m
0.048	2.5	83	2.2
0.051	3.6	84	2.3
0.064	4.3	145	2.3
0.067	4.2	169	2.23
0.075	4.5	165	2.5
0.11	5.2	581	2.9
0.114	5.5	1217	3

Finally, it is worth mentioning that incorporating fillers, such as nanoclays [68,89], carbon nanotubes [90] or graphite particles [74,91] in the tannin-based formulation before foaming, polymerisation and pyrolysis is easy and allows obtaining composite foams. For instance, since the thermal conductivity of tannin-based char is rather low (slightly less than 4 W/m/K), the corresponding carbon foams are rather insulating. In the domain of seasonal heat storage, higher conductivities but still high porosities are required for transferring the heat to/from phase-change materials hosted in graphite foams. However, the conductivity should not be too high either, so that graphite foams proved to be irrelevant (see the specifications that such foams should have in [92]). A moderate thermal conductivity can therefore be obtained by preparing composite foams based on tannin-derived char as matrix and graphite flakes as

filler. The presence of graphite particles made the formulations more viscous and thus limited the foaming and the development of cells, but increased the thermal conductivity by more than one order of magnitude while maintaining a very high porosity, still relevant for hosting phase-change materials with a high volume energy density [74,91]. This excellent performance was achieved using natural graphite flakes with an optimal size of 6 µm.

All these results demonstrate that model carbon materials can be prepared from tannin, based on which new knowledge in physics can be gained by validating models successfully applied to concrete situations.

3.2 Other biosourced cellular carbons

3.2.1 *Monoliths derived from colloidal systems*

Beyond foams, other cellular carbons were produced from tannin-based colloids. The first way was, by borrowing a term from the culinary vocabulary, to prepare a "mayonnaise", i.e., an oil-in-water emulsion. Adding dropwise vegetable (sunflower) oil to an aqueous solution of tannin (with surfactant, crosslinker and catalyst) and stirring the whole led to an emulsion, which was subsequently polymerised in an oven and whose oil was removed by extensive washing in a Soxhlet extractor (Figure 6(a)). It was also possible to use a volatile, water-immiscible solvent such as cyclohexane, which, by simple evaporation, led to identical structures but with typically 10 times smaller cell sizes. The resultant polyHIPE (polymerised High Internal Phase Emulsion), whose pore size and connectivity could be tuned by the initial volume fraction of oil, was then pyrolysed [93,94]. The "carboHIPE" thus obtained proved an interesting metal-free electrocatalyst for the oxygen reduction reaction (ORR) when tested in alkaline conditions. Especially, one of these materials (CFAT-C in Figure S4(a-d)) presented a number of electron transfer close to 4, an onset potential close to that of Pt/C, and a high

stability to methanol addition and to cycling [95]. A SEM picture of this material is provided in S4(e).

These encouraging results and the in-depth studies of the corresponding carbons suggested the following ORR mechanism: oxygen groups at the surface of large pores promote the transport of O_2 dissolved in the electrolyte to very narrow pores having hydrophobic surfaces and high adsorption energy. Therein, strong physical adsorption forces and charge transfer from the carbon surface to adsorbed O_2 weaken the O–O bond and favours O_2 dissociation and hence its reduction to water. The latter is then easily expelled from the narrow, hydrophobic pores, and the process can be repeated [95].

A second way to prepare cellular carbons, though still rather similar to the previous one, was to beat strongly the emulsion so that the latter was progressively aerated into what we may call a "Chantilly cream", using the same culinary analogy as before [93]. As a result, carbons with hierarchical porosity are obtained, i.e., having the same small cells as before due to the removal of the oil droplets from the emulsion, but also big cells due to the incorporation of air bubbles in the emulsion. More oil in the emulsion increases its viscosity, and consequently the big pores formed by bubbles are smaller (see Figure 6(b)).

(a)

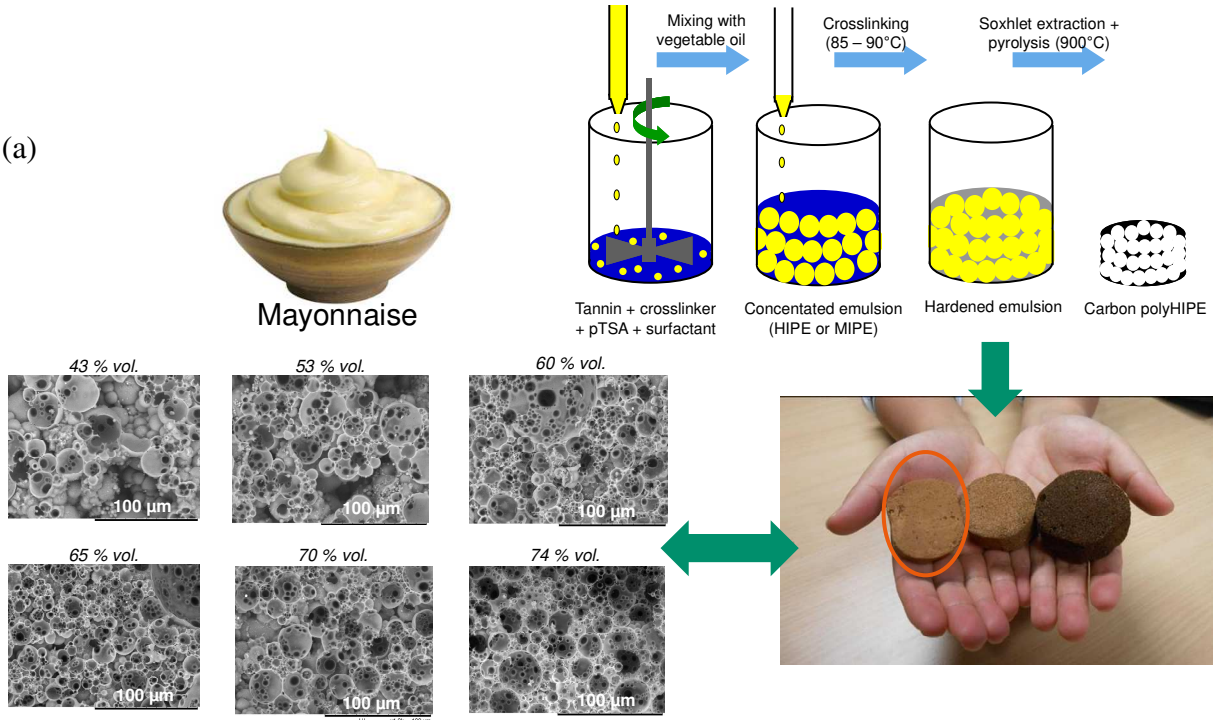

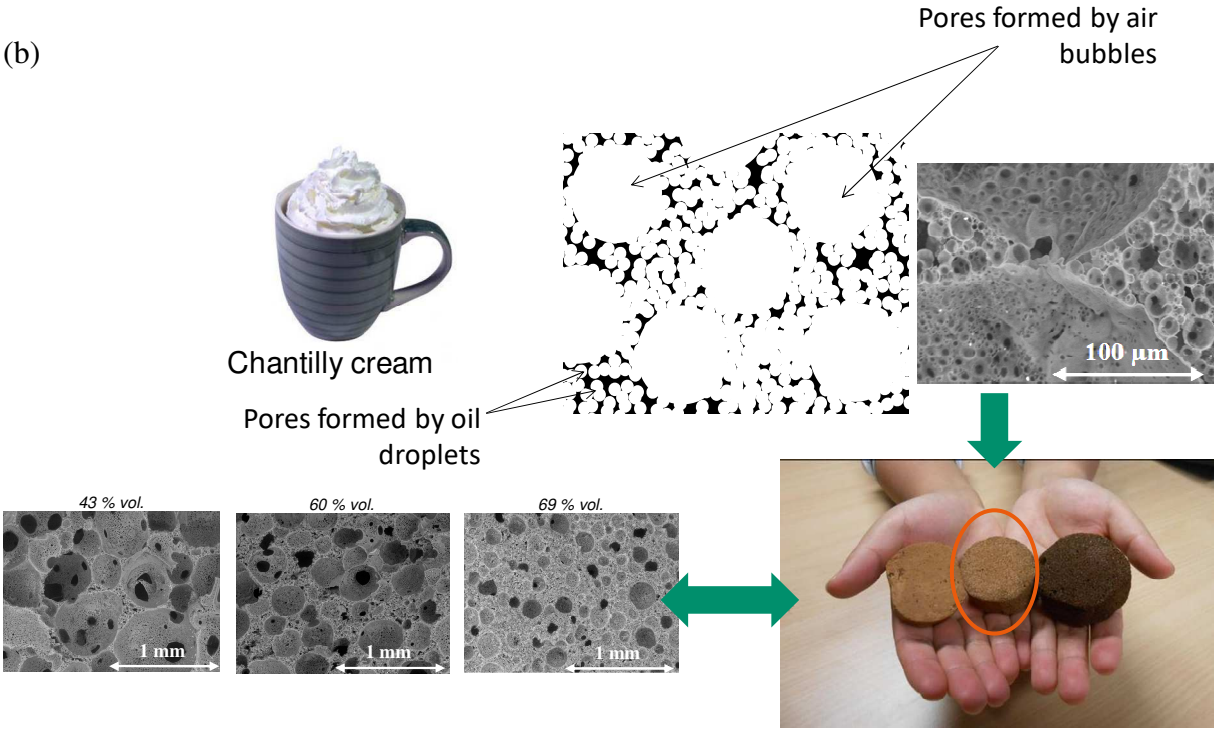

Figure 6. General preparation scheme and structure of tannin-based cellular carbons derived from: (a) emulsions, and (b) aerated emulsions, containing various volume fractions of oil. (Adapted from [93,94] with permission from Elsevier).

Finally, the former method can be used even in the absence of emulsion, provided that surfactant is present. By just whipping until stiff the same aqueous solution of tannin containing polymerisation catalyst and crosslinker, a liquid foam that can be polymerised in an oven is obtained, leading to what we call “meringue” by continuing the culinary analogy. This time, the cell size is controlled by the concentration of tannin in the solution that was whipped, higher concentrations leading to higher viscosities and hence to smaller cells (see Figure 7) [93,96]. After pyrolysis, the resultant “carbon meringue” was investigated as metal-free catalyst for ORR, as such or after chemical modification by doping with either N or S, and in the presence or not of graphene oxide as additive. The results (Figure S5) supported the ORR mechanism already considered with the tannin-based carboHIPEs, and confirmed the

very important role of hydrophobic micropores as catalytic centres. The electrocatalytic properties were even better than before, with a number of electrons transferred much closer to 4 and with an increased stability to cycling. The beneficial role of doping was also highlighted, provided that such chemical modification does not significantly decrease the availability of the narrow microporosity [97].

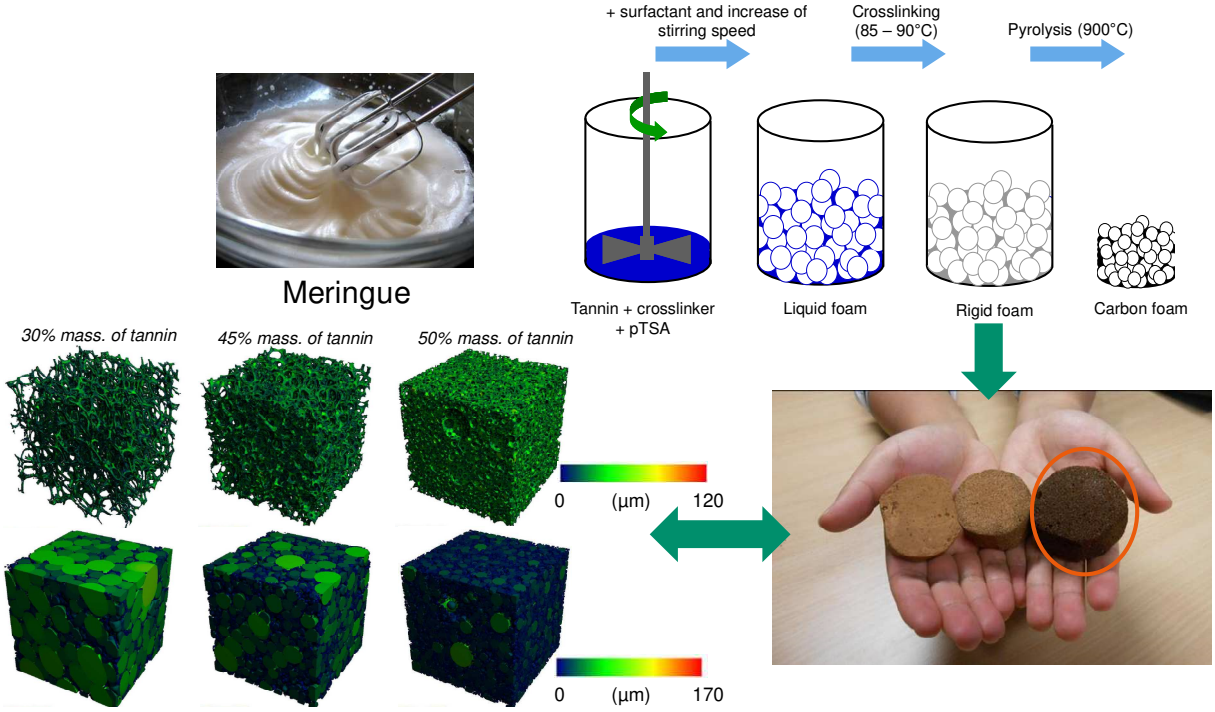

Figure 7. General preparation scheme of tannin-based cellular carbons derived from liquid foams obtained by whipping aqueous solutions, showing the structure as seen by tomography as a function of the initial tannin concentration (top: view of the solid backbone, bottom: view of the pores) (Adapted from [93,96] with permission from Elsevier).

Other counterintutive cellular carbons, in the sense that their cell size increases with their bulk density (i.e., exactly the opposite of what is encountered in most foams) were also prepared from tannins. In this case, sacrificial templates made of paraffin spheres of controlled diameter were compactly stacked in a container in which a tannin-based resin was poured and polymerised. Next the paraffin spheres were dissolved, and the remaining cellular

solid was pyrolysed. The results are shown in Figure 8, where SEM pictures of monoliths of increasing density are seen from left to right, and where playing with the two electron detectors of the SEM proved very useful with this kind of material. The secondary electron (SE) detector indeed allows seeing cell walls very clearly, whereas the backscatted electron (BSE) detector allows seeing the windows connecting the cells. Based on such images, it was possible to demonstrate the existence of cellular materials in which bigger cells correspond to lower porosity, therefore compensated by thicker cell walls. Just like for the former model vitreous carbon foams, the dc electrical conductivity was found to be independent from cell size, and the classical power law with the effective-medium exponent ½ was recovered, by which the conductivity of non-porous vitreous carbon could be estimated [73].

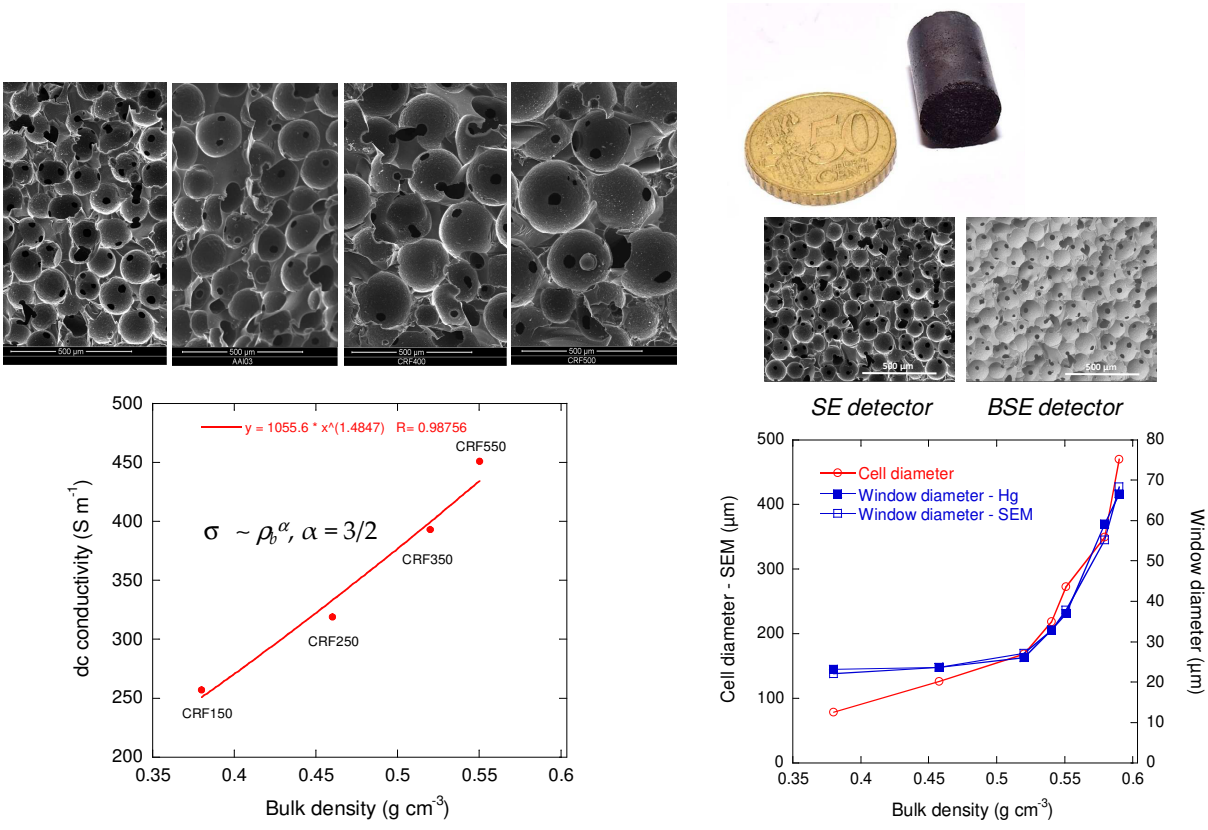

Figure 8. Tannin-based cellular carbons prepared from templating with sacrificial (paraffin) spheres: SEM pictures (top left, with a scale bar of 500 µm) at the 4 different densities

indicated in the plot of electrical conductivity (bottom left), real-size monolith (top right), views of the same material through the use of two different electron detectors (see text), and dependance of cell and window sizes on bulk density (bottom right). (Adapted from [73] with permission from MDPI).

3.2.2 *Monoliths derived from additive manufacturing*

3D printing is a powerful tool for building complex structures. However, carbon can obviously not be processed directly, and either need to be produced by pyrolysis of a 3D-printed preform, or be processed in the form of a powder in the presence of a binder that can be carbonised afterwards. In the present case, non-fusible preforms were produced by stereolithography of photocurable polymers, which were subsequently coated by hydrochar produced by the polycondensation and dehydration in hydrothermal conditions of an aqueous solution of tannin containing a significant amount of dissolved nickel sulphate. The latter proved to be necessary for enhancing the carbon yield of the structures after pyrolysis, and for avoiding its deformation [98]. As a result, partly graphitised periodic carbon structures were obtained, in which the polymer preform was destroyed but very efficiently replicated by the process of hydrochar deposition and carbonisation (see Figure 9).

For easier handling the carbon structures, whether based on Kelvin cells or on Gibson-Ashby cells, the sample were impregnated with epoxy resin and tested in waveguides for studying their electromagnetic properties in the GHz-THz range (see Figures S6(a) and S6(b)). The materials were found to behave as photonic crystals in this range of frequencies, and the modelling predicted an abrupt change from an almost completely reflecting behaviour in the GHz domain to an almost purely absorbing behaviour in the THz, with a crossover frequency depending on the characteristic cell size of the periodic structures. This behaviour was indeed observed when measuring the materials in the THz range (see Figure S6(a)) [99].

Over the full range of investigated frequencies, the transmittance (i.e., 1 – absorbance – reflectance) of the materials was strictly zero.

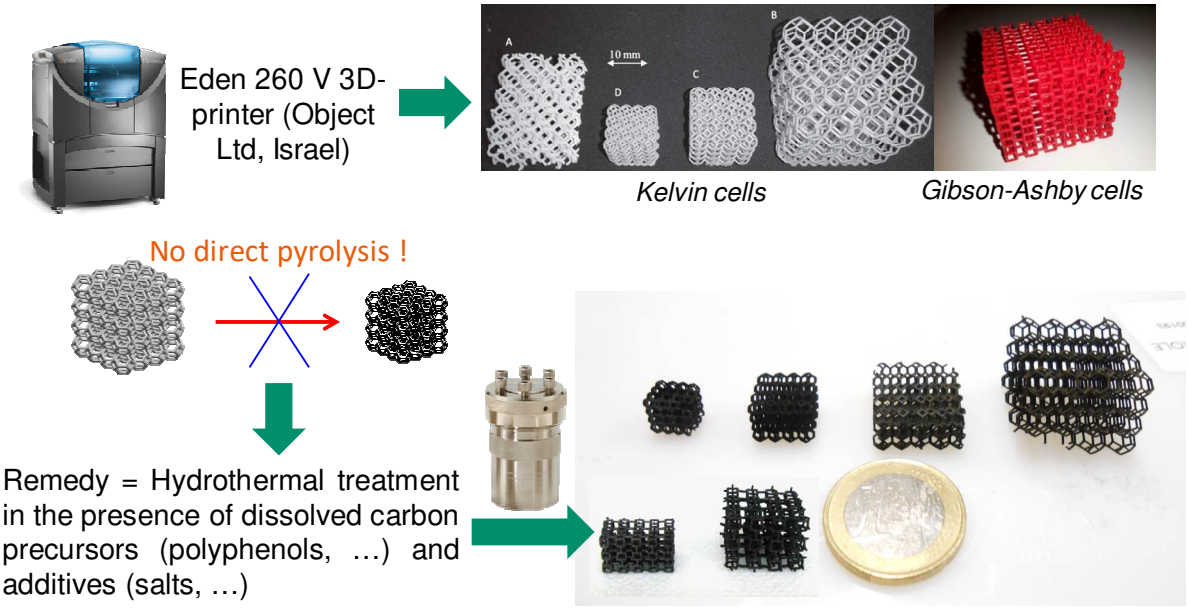

Figure 9. General preparation scheme of tannin-based periodic carbon structures (Reprinted from [98] with permission from Elsevier).

The distribution and intensity of the electric field in carbon periodic structures based on Gibson-Ashby cells submitted to electromagnetic waves in the GHz range could also be successfully modelled: see Figure S6(b), where each coloured line corresponds to a constant value of electrical field averaged over all phases. Such modelling was able to predict not only the frequency of the peak of absorption (i.e., the minimum of reflection in Figure S6(b)), but also its progressive shift depending on the strut thickness (at constant cell size, bottom left of Figure S6(b)) and on the dielectric constant of the medium filling the carbon cells (bottom right of Figure S6(b)) [99].

3.2.3 *Packing of hollow carbon spheres*

Finally, cellular carbons are not only monolithic but can take the form of lattices based on hollow carbon spheres. The latter were obtained in the same way as the aforementioned 3D periodic structures, i.e., by using aqueous tannin solution in hydrothermal conditions and in the presence of metal salts. The templates were either polymer capsules filled with sugar alcohols or just fish eggs (lumpfish roe) [100]. In the latter case, after the eggs were thoroughly washed for removing the brine in which the roe was kept fresh, it was possible to adjust both the diameter and the shell thickness of the final hollow carbon spheres. For that purpose, the nature and the amount of metal salt dissolved in the hot pressurised aqueous solution in which the roe was hydrothermally treated were changed (see top of Figure 10(a)). Salts from the Hofmeister series are indeed known to start from kosmotropes (with a salting-out effect, i.e., preventing protein denaturation and leading to less soluble polymers) and end with chaotropes (with a salting-in effect, i.e., helping protein denaturation and leading to more soluble polymers) [101]. Another way consisted in choosing one salt, KF at the bottom of Figure 10(a), and increasing its concentration in the autoclave, which produced, after pyrolysis at 900°C, hollow carbon spheres with gradually lower diameter and shell thickness.

Based on the inspiring strategy of the moth-eye structure (see Figure 10(b)), known to behave as a non-reflecting surface in the visible light, a 2D dense packing of hollow carbon spheres was prepared (Figure 10(c)). The latter indeed behaved as a metasurface with almost 100% of absorption in the microwave range, as expected given the much larger diameter of the present spheres, and the modelling of the results (Figure 10(d)) allowed predicting optimal values of diameter and shell thickness. The same kind of spheres, obtained with different diameters and from different carbon sources (Figure S7(a))), in the presence or not of graphitisation catalysts such as Fe or Ni, were also tested as floating bodies to boost the solar

evaporation of water. Submitted to a solar simulator, the best materials were those of maximum diameter and floating below the water surface, therefore maximising the contact area between carbon and water, and tannin was found to be a more efficient carbon source than sucrose for that purpose (see Figure S7(b)). The incorporation of iron or nickel graphitised the carbon and gave the spheres a strong ferromagnetic character, thereby making their recovery from water very easy (Figure S7(c)). These carbon spheres proved floating for more than 3 months, after which the experiments were stopped [102].

(a)

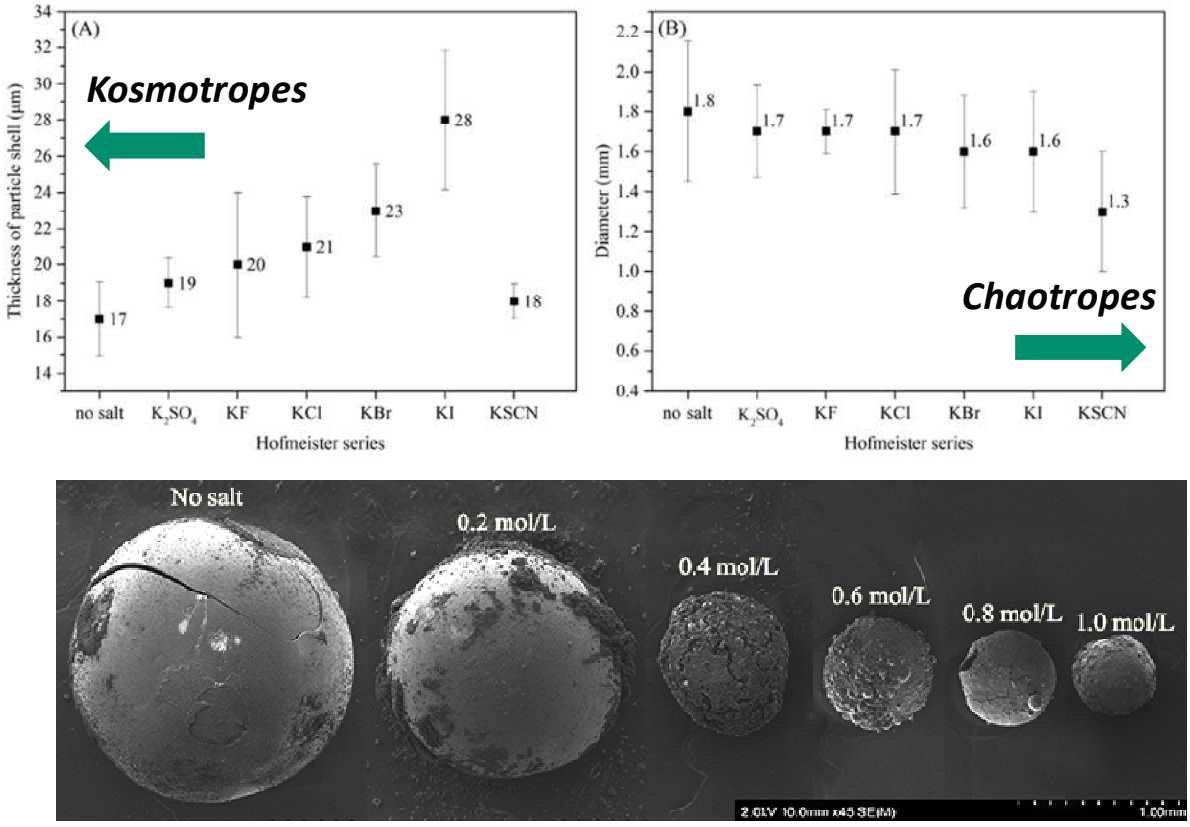

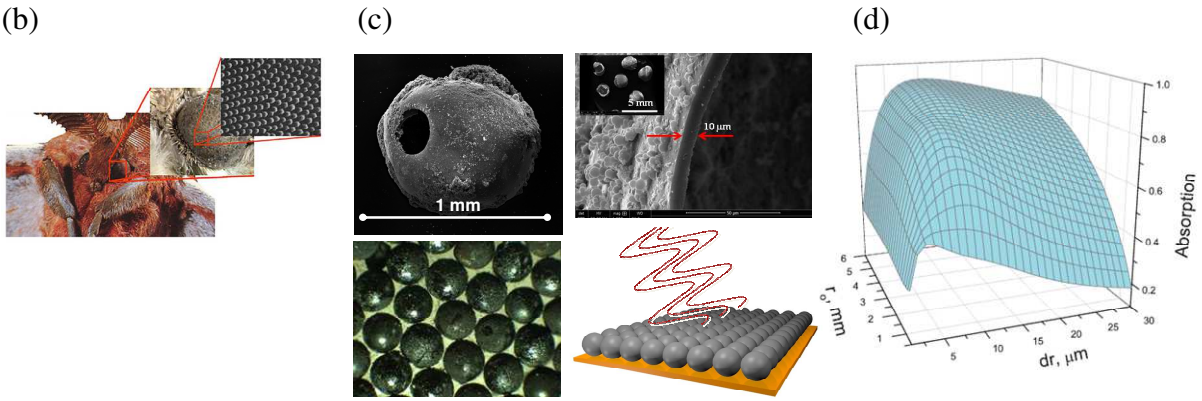

Figure 10. (a) Changes of geometrical parameters of hollow carbon spheres obtained by pyrolysis at 900°C of fish eggs treated in hydrothermal conditions in the presence of tannins with either various salts at constant concentrations (top) or with KF at increasing concentration (bottom); (b) Inspiring strategy based on the moth-eye structure for preparing non-reflecting metasurfaces; (c) Hollow carbon spheres (top: a broken one was deliberately chosen for showing the hollow interior) and resultant biomimetic metasurfaces based on them (bottom); (d) Modelling of the electromagnetic response of a 2D packing of hollow carbon spheres, showing optimum values of diameter and shell thickness for reaching nearly 100% of microwave absorption. (Adapted from [101] with permission from Wiley and from [100] with permission from AIP Publishing).

4. Mesostructured carbons

4.1 Ordered mesoporous carbons from hard-templating

Hard-templating, also called nano-casting, is a well-known method consisting in impregnating a mesoporous structure (the template) by a carbon precursor, carbonizing the whole, and dissolving the template for recovering the corresponding carbon replica [103–107]. Here the originality was the use of condensed tannins and tannin-related molecules such

as, by increasing order of size, phloroglucinol, gallic acid, and catechin. It was indeed not obvious at all that the biggest molecules would successfully impregnate an SBA-15 mesoporous silica to produce flawless carbon mesostructures. Although it is true that condensed tannins (Ta in Figure 11) indeed led to the lowest yield, the latter was, however, only slightly lower than what was obtained with the other molecules, especially with catechin, which is the basic structural unit of mimosa tannin. After removing the silica, all biosourced precursors led to ordered mesoporous carbons (OMCs) having the same hexagonal structure (space group P6mm), with a mesopore diameter centred on 3.4 nm.

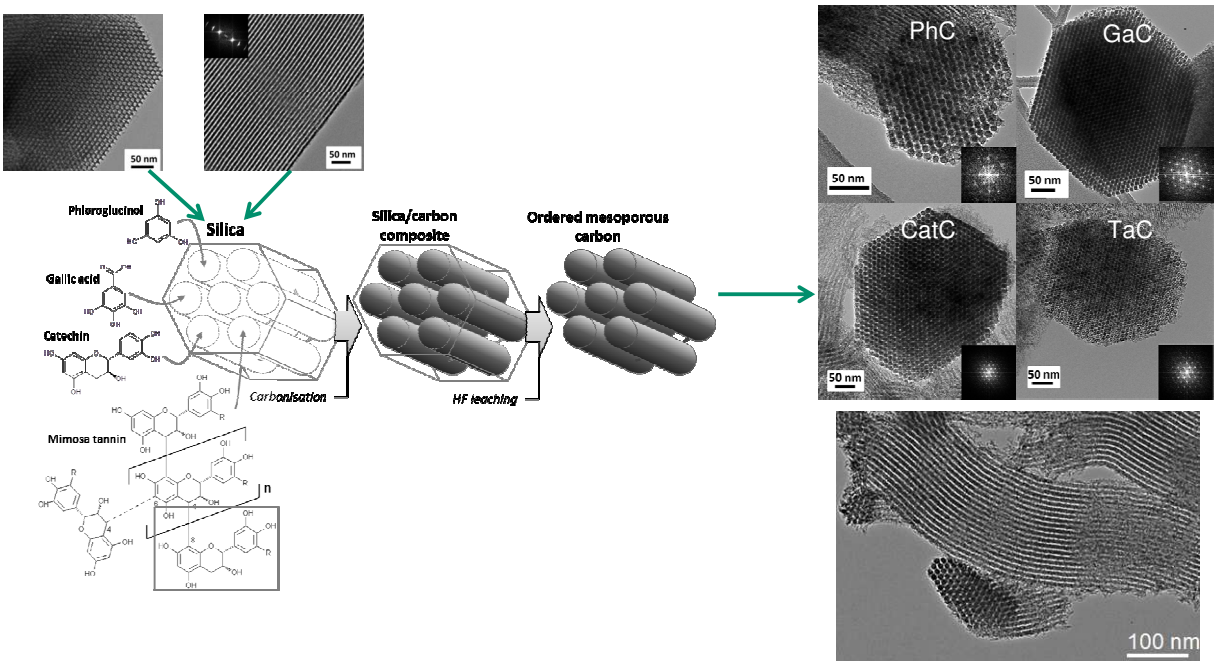

Figure 11. Preparation of ordered mesoporous carbons (OMCs) by nano-casting using SBA-15 mesoporous silica as template (top left: TEM cross-section and longitudinal views), biosourced precursors (phloroglucinol (Ph), gallic acid (Ga), catechin (Cat) and condensed mimosa tannin (Ta)), and resultant OMCs after removal of silica (top right: TEM cross-section views; bottom right: longitudinal view) (Reprinted from [108] with permission from Elsevier).

Although the structures were qualitatively the same, N_2 and CO_2 adsorption revealed differences of micro and mesopore volumes, as seen in Figure S8(a). Testing the materials as supercapacitor electrodes in a two-electrode cell system evidenced electrochemical performances higher than those of other OMCs prepared by CVD-infiltration of SBA-15 silica (see Figure S8(b)) [108].

4.2 Ordered mesoporous carbons from soft-templating

Soft-templating is a green preparation method since no corrosive chemicals are required for removing the hard template [109–113]. In this method, amphiphilic surfactants auto-organise into micelles, around which the polymerisation of a biosourced resin takes place. After crosslinking, a simple pyrolysis converts the resin into carbon while the micelles, which start decomposing at 400°C, are completely volatilised at 900°C, leaving behind an ordered lattice of mesopores having controlled size and geometry. Consequently, whereas the former OMCs were based on solid rods connected by thinner ones, the present OMCs have the inverse structure, i.e., are porous carbons with tubular, parallel mesopores. Such materials could be prepared by evaporation-induced self-assembly (EISA method, see Figure 12(a)), leading to OMCs having a hexagonal structure (space group P6mm) with a mesopore diameter centred on 7.2 nm [114], or by phase separation (see Figure 12(b)), producing OMCs having the same structure but a mesopore diameter centred on 6.5 nm [115].

These materials were successfully tested as supercapacitor electrodes, and the development of their microporosity by activation with CO_2 improved their performances further. The resultant material indeed presented, for instance, a remarkably stable 90% of capacitance retention even after 5000 cycles [116]. The materials were also investigated as photocatalysts for the degradation of rhodamine B and, interestingly, the photoactivity determined from

kinetic measurements was found to be linearly dependent of the volume of supermicropores [117].

(a)

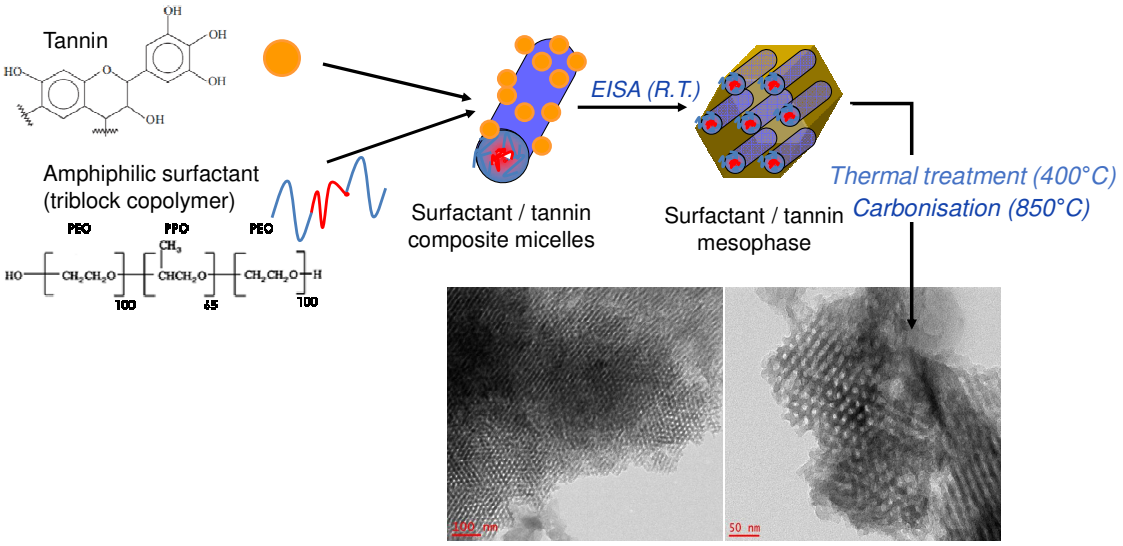

(b)

Figure 12. General preparation scheme and structure of tannin-based OMCs obtained by soft-templating, and corresponding TEM pictures of their structures: (a) Evaporation-induced self-assembly (EISA) method; (b) Phase-separation method. (Reprinted from [114] and from [115] with permission from the Royal Society of Chemistry).

A new route based on mechanosynthesis was developed in 2018, which is much faster and greener since it requires only 1h (instead of 36h and 60h for EISA and phase separation methods, respectively), and since no acid or formaldehyde is needed either. Tannin is simply

mixed with the same amphiphilic surfactant as before, and the mixture is ball-milled in the presence of a little amount of water only. This produces the formation of a mesophase, by which the tannin resin is mesostructured and maintains its structure during pyrolysis (see Figure 13(a)). The method is highly versatile because, depending on the relative amounts of water and surfactant, different kinds of mesostructuration can be obtained: either perfectly ordered OMCs with a single mesopore size on the one hand, or disordered mesoporous carbons also having a single mesopore size but with a wormlike mesopore structure on the other hand. In addition, using other preparation conditions, either bimodal (i.e., micro-mesoporous) OMCs or purely microporous carbons could also be obtained. Figure 13(b)) thus presents the phase diagram in the water (W) – surfactant (P for "Pluronic® F127") system, in which different zones are seen with examples of pore-size distributions. The centre of the contour lines corresponding to the maximum ratio amplitude / FWHM of the pore-size distribution led to the sample with the most ordered and single-sized mesoporosity [118].

(a)

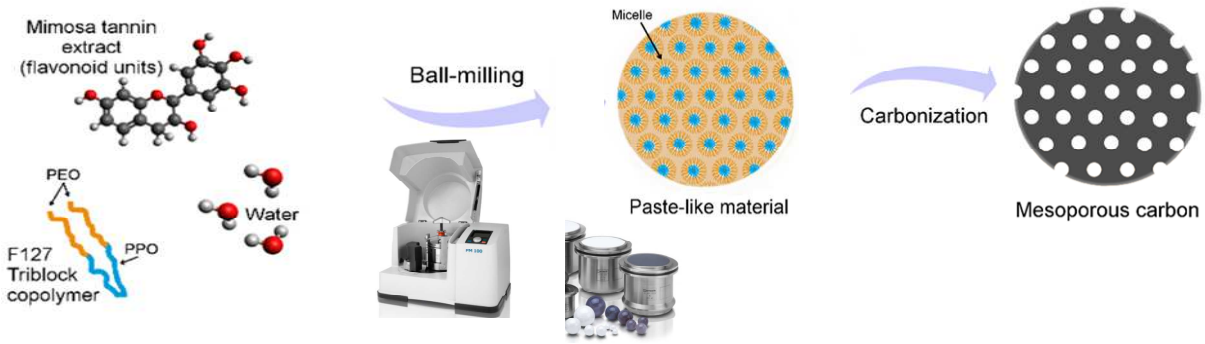

(b)

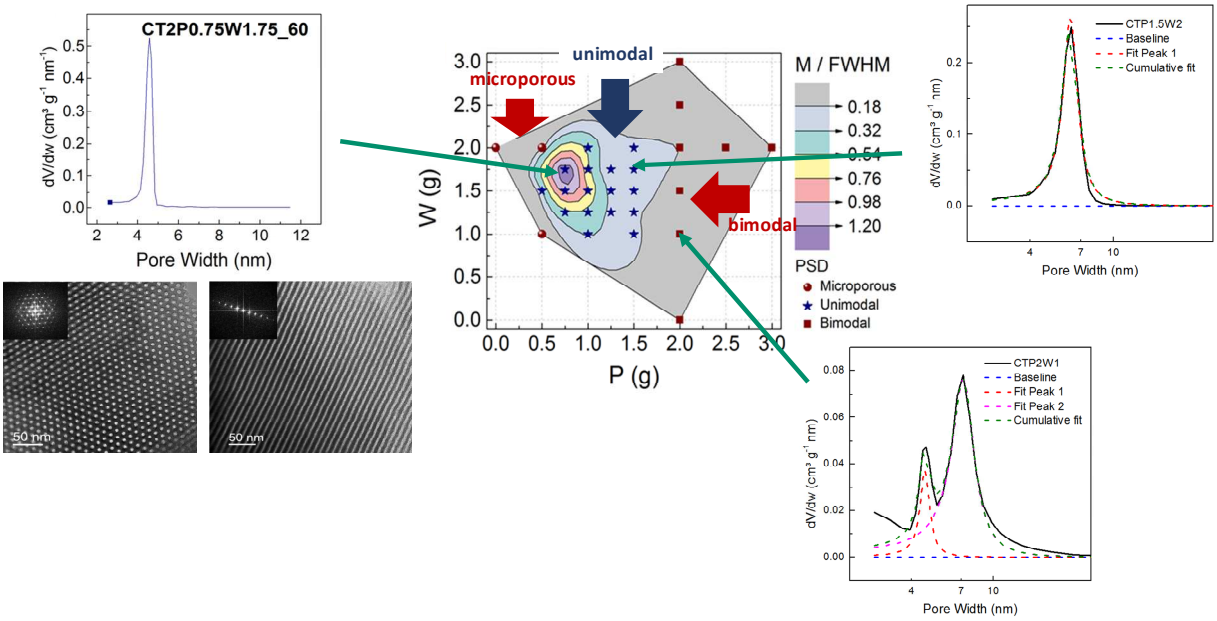

Figure 13. (a) General preparation scheme and structure of tannin-based OMCs based on water-assisted mechanosynthesis in the absence of polymerisation catalyst and crosslinker; (b) Examples of materials found in the water – surfactant phase diagram (see text) based on their pore-size distribution, and TEM cross-section and longitudinal views (bottom left) of the material having the most ordered and single-sized mesoporosity (Adapted from [118] with permission from the Royal Society of Chemistry).

These OMCs maintained their mesoporosity whatever the heat-treatment temperature and after physical or chemical activation. Without treatment, they proved to be extremely hydrophobic materials (water contact angle higher than 157°) and were very efficient for selectively trapping, within a few seconds only, hydrocarbons such as heptane spread at the surface of water [118]. The same feature, associated with a rather high packing density, makes them very interesting for capturing CO_2 in real conditions, i.e., from wet and hot (> 75°C) gaseous streams [119]. Activation dramatically increased the surface area and both the connectivity between micropores and mesopores and the oxygen content at the material

surface. As a result, an adequate balance between high surface area and relevant pore-size distribution was met for reaching excellent performances as supercapacitor electrodes in aqueous and organic electrolytes. In particular, high specific energy and power were obtained, as well as high-rate capability with capacitance retentions (70% at current densities as high as 80 A/g) and very good long-term stability over time and after continuous cycling under realistic testing conditions [120].

Finally, these materials are highly valuable subjects of research because their mesoporosity can be either perfectly ordered or disordered at one constant mesopore size, and therefore their tortuosity, connectivity and mesoporous surface area can be tuned and investigated by different methods. They thus appear as model materials, much like the model foams described in section 3.1, and on which it is again possible to compare reliable experimental measurements with theoretical predictions related to, for instance, adsorption of gases and electron tomography. The former may indeed, by scanning the hysteresis loop of nitrogen adsorption-desorption isotherms, give information on the phenomena that take place during desorption, such as cavitation, pore blocking or percolation effects. Regarding electron tomography, reconstruction algorithms are presently used based on series of TEM images obtained by tilting the sample gradually in a broad range of angles. The corresponding reconstruction of 3D images thus allows computing many quantities of interest, such as porosity, aperture size distribution, pore morphology, constrictivity, coordination number, tortuosity, etc. These reconstruction algorithms can be refined and calibrated based on accurate adsorption results. The same set of numerical data can also be used for improving molecular simulations used to build realistic porous materials structures and predict their physical properties in terms, for instance, of diffusivity, with applications in gas separation, capture and storage, as well as in catalysis. There is thus a unique opportunity offered by

these mesoporous carbons to improve our knowledge and understanding of phenomena taking place in nanopores. This work is in progress, and the molecular sieving effect of OMCs has already been demonstrated for separating isomers of linear from branched hydrocarbons with an exceptional efficiency [60].

5. Carbon gels

5.1 Tannin-based counterparts of classical aero, cryo- and aerogels

Just like the most well-known precursors of carbon gels, phenol and especially resorcinol, condensed tannins can be gelled in more or less diluted solutions and lead to the same materials with a cost about 5 times lower, while having many other advantages. Tannins are indeed much more versatile in the sense that they react with a number of crosslinkers over the entire pH range while requiring less of them at the same time (especially formaldehyde), and in various protic solvents. Additionally, they are miscible in all proportions with phenol or resorcinol and react with each other (i.e., it is not just a blend of different molecules but truly mixed oligomers), making the resultant materials much greener [71,121–124]. They can also produce mixed gels with many other molecules, of natural origin (tannin-lignin [125], tannin-soy proteins [126]) or not (triblock copolymers [127]).

And obviously, once the organic gels are formed, they can be dried in different ways and lead, after pyrolysis, to either carbon aerogels, cryogels or xerogels. The porosity can be narrowed by increasing the pH of preparation, just as for classical syntheses based on resorcinol. Another way of tuning the porosity is incorporating different amounts of triblock copolymers in the formulation, making possible to achieve bimodal pore-size distributions (see Figures 14 and S9) [72]. A remarkably broad range of porous structures can therefore be

achieved, within which it is possible to find either materials having different pore-size distributions at roughly constant pore volumes, or a fixed pore-size distribution but very different pore volumes. Much more about the broad topic of tannin-based carbon gels can be found in a recent monograph [56].

Tannins could also be used in what is probably the cheapest and easiest way of synthesising carbon molecular sieves. For that purpose, microspheres are prepared by gelation in suspension, i.e., by introducing dropwise a tannin-formaldehyde-surfactant solution into sunflower oil under stirring. As seen in Figure 15, their mean size after solvent exchange with pure ethanol, simple drying in air and pyrolysis at 900°C depends on both stirring speed and concentration of surfactant, so that the smallest microspheres had a diameter close to 15 µm (at the highest stirring speed and amount of surfactant) [70]. Most of these microspheres, depending on their synthesis parameters, presented very narrow micropore size distributions (see again Figure 15). The latter was indeed centred on 0.5 nm for most materials, and almost no mesoporosity was present. These materials should thus be suitable as very cheap and green carbon molecular sieves.

The general cheapness of tannin-based carbons was also evidenced when synthesising activated carbon gels: an innovative yet very efficient way of developing the microporosity of these materials was demonstrated by simply impregnating tannin-based hydrogels by aqueous solutions of NaOH or KOH, followed by drying and pyrolysis at 750°C. Surface areas as high as those obtained in usual syntheses using carbon xerogels as precursors of activated carbon were thus achieved by using about 5 times less alkali hydroxide (see Figure S10) [128].

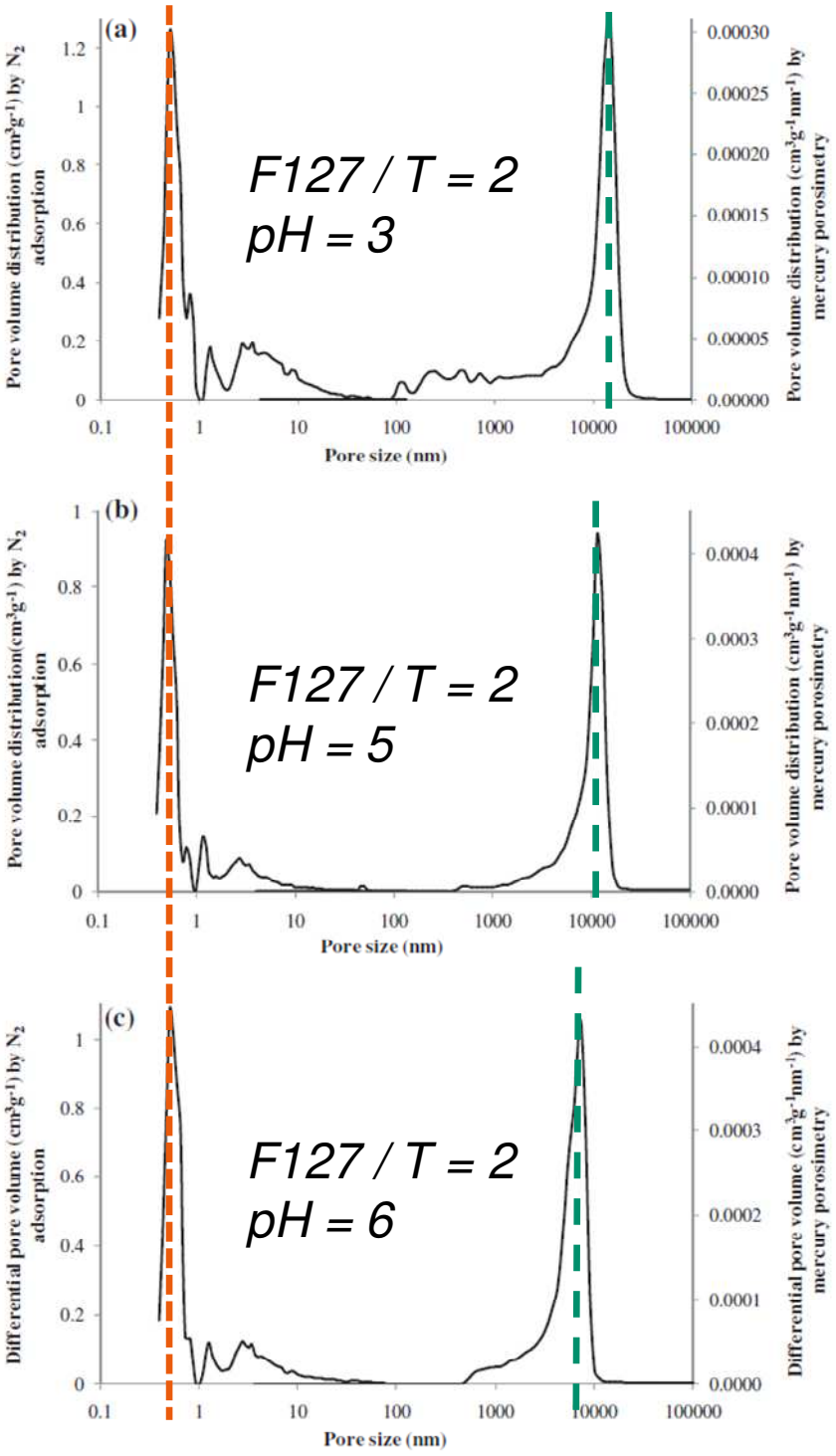

Figure 14. Pore-size distributions (from N_2 adsorption and Hg porosimetry) of tannin-based carbon xerogels prepared at pH 3, 5 and 6 with a weight ratio of triblock copolymer (F127) to

tannin of 2: whereas the microporosity is unaffected, the macroporosity becomes narrower as the pH increases (reprinted from [72] with permission from Elsevier).

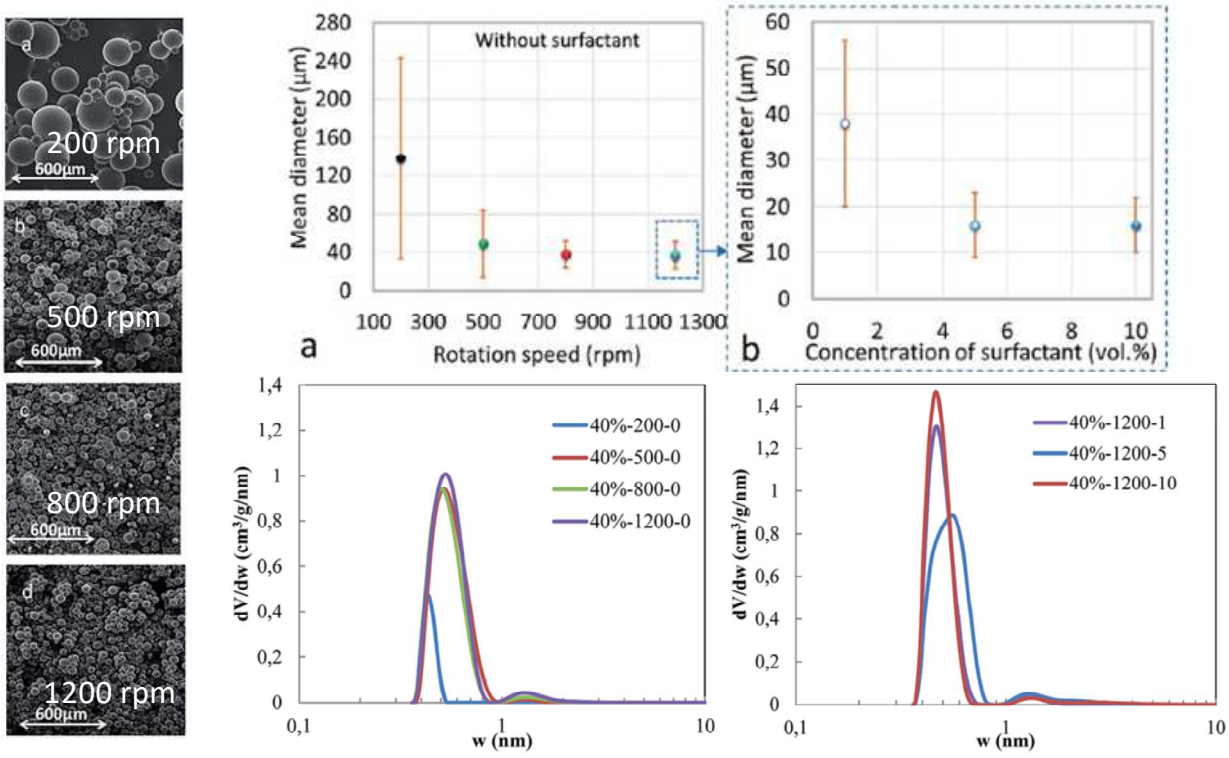

Figure 15. Tannin-based carbon molecular sieves: SEM pictures of carbon xerogel microspheres (prepared without surfactant and at different stirring speeds) and corresponding changes of mean diameter and pore-size distributions as a function of synthesis parameters (stirring speed and surfactant concentration) (reprinted from [70] with permission from the Royal Society of Chemistry).

5.2 Formaldehyde-free carbon gels

One more exceptional feature that tannins may show is the possibility of gelling in amazingly short times at room temperature, within minutes and even within a few seconds only with some formulations, thereby making the synthesis of carbon gels not much longer than the only final pyrolysis step. In contrast, gelation of resorcinol usually takes several days at temperatures close to 80°C. Figure 16(a) shows the example of carbon gels made by auto-

condensation of tannins catalysed by silica [129]: adding waterglass to a tannin solution induces its gelation in about 2.5 min at room temperature, and the subsequent supercritical drying with CO_2, pyrolysis at 900°C and dissolution of the nano-silica trapped inside (either with HF or NaOH solutions) led to more porous carbon aerogels than those prepared by the classical route where tannins are crosslinked with formaldehyde during 5 days at 85°C. The resultant materials are highly mesoporous with surface areas as high as 780 m^2/g.

Another way of producing crosslinker-free (and hence formaldehyde-free) carbon gels is the ability of tannins to react with concentrated ammonia. The multi-amination of the hydroxyl groups of tannins, as well as the spontaneous oligomerisation and crosslinking through –N= bridges that result not only introduces N in the structure of these carbon precursors[130], but also induces the gelation of aminated tannin into N-doped carbonaceous hydrogels (Figure 16(b)) [131]. Such hydrogels, whose porous texture depends on the amount of materials introduced in the autoclave used for the hydrothermal treatment, can be next dried in normal conditions, or freeze-dried, or dried in supercritical conditions and finally pyrolysed, leading to N-doped carbon xerogels, cryogels or aerogels, respectively (Figure S10) [132]. Despite their moderate surface areas close to 500 m^2/g, carbon xerogels contain about 3 and 16 wt.% of N and O, respectively, thus facilitating Faradaic reactions and hence explaining their quite high normalised capacitance, near 60 $\mu F/cm^2$ [133].

(a)

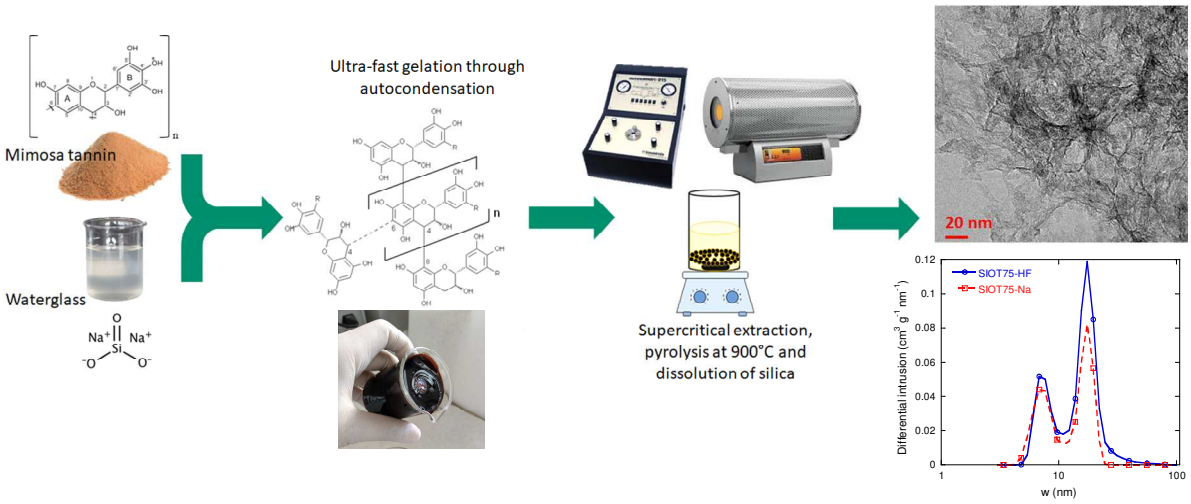

(b)

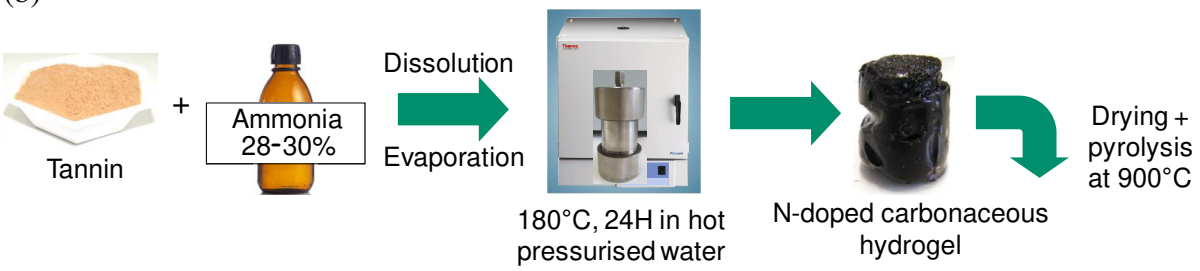

Figure 16. Formaldehyde-free tannin-based carbon gels: (a) General preparation scheme, TEM picture and pore-size distribution of carbon aerogels prepared by autocondensation of tannin catalysed by silica, after silica dissolution by either HF or NaOH solutions; (b) General preparation scheme of N-doped tannin-based carbonaceous hydrogels (adapted from [129] with permission from KeAI Publishing).

6. Miscellaneous tannin-based materials

6.1 Hydrothermal carbons and related materials

Since tannins are soluble in water, it is easy to force their condensation and dehydration by placing them in hot pressurised water, typically at 180°C for 24h. Then, much like to what is well known for sugars, hydrothermal carbon is produced (1st order kinetics, activation energy

91 kJ/mol [134]), and the minimisation of its surface energy makes it appear in the form of microspheres (see Figure 17(a)), with an excellent yield, close to 60%. In addition to time and temperature, these particles are sensitive to the pH and to the presence of dissolved metal salts [135,136]. This matter of fact is related to the influence of pH on the kinetics of tannin auto-condensation reactions, and to the ability of tannin to complex transition metals. The reactivity of tannin also allows reaching very high N levels when treated in an autoclave containing a 28 wt.% ammonia solution, leading to carbons having BET areas of about 500 m^2/g and N contents of 8 wt.% after pyrolysis at 900°C. This is an exceptional combination of values, since pyrolysis at such high temperature usually decreases the N content to much lower levels, and that high N contents are generally found in carbons of much lower surface areas [137].

(a)

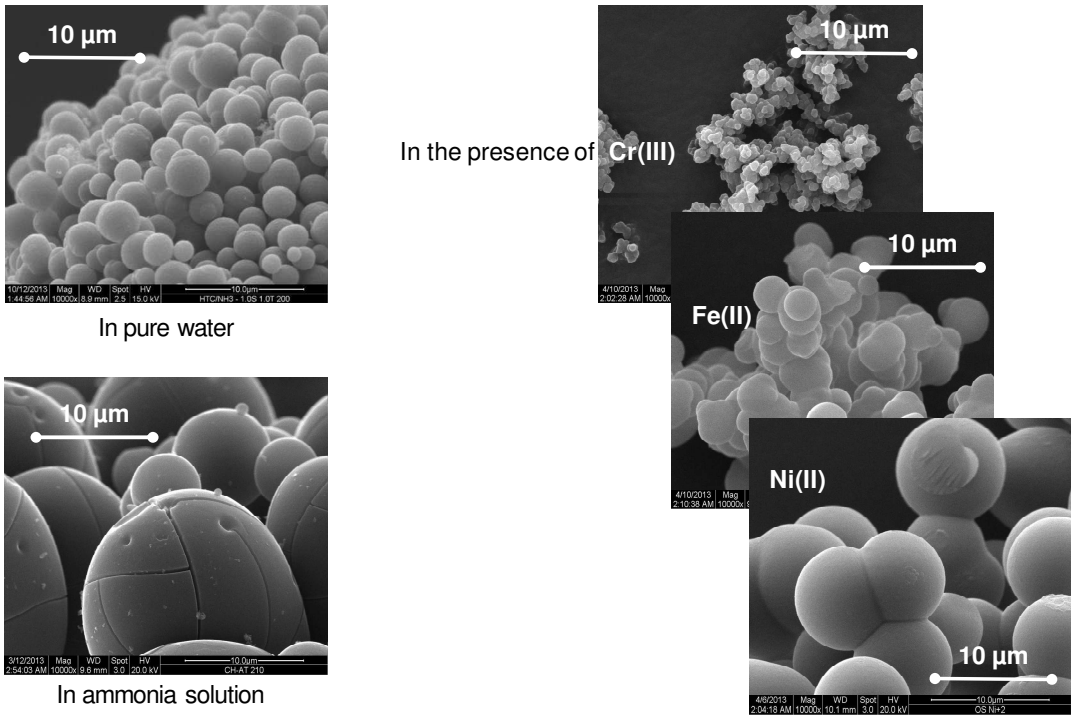

(b)

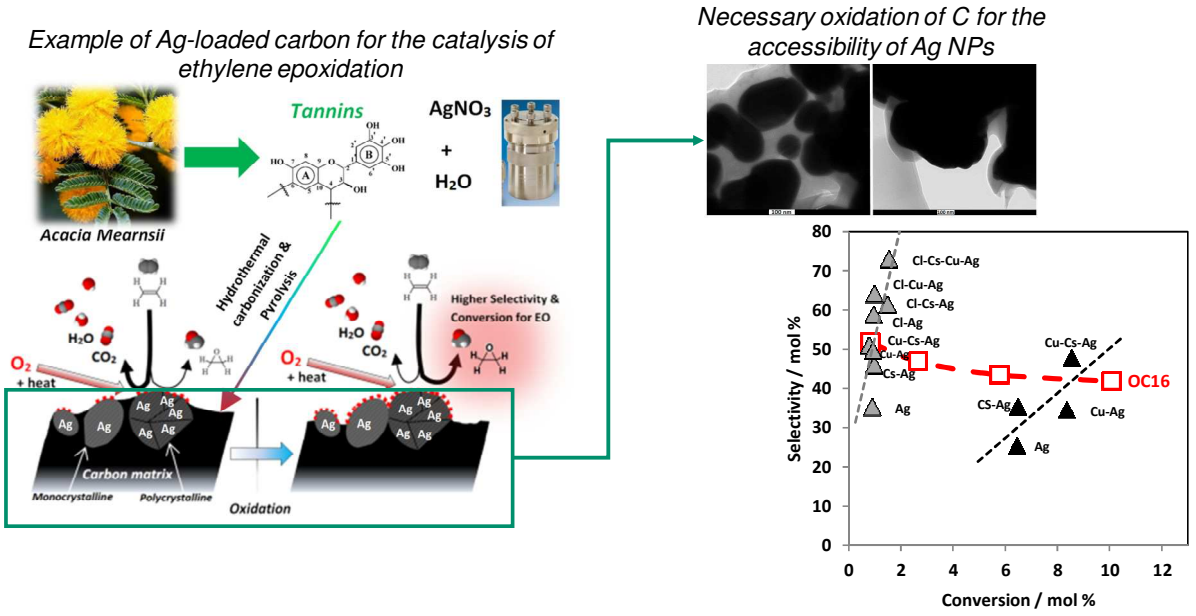

(c)

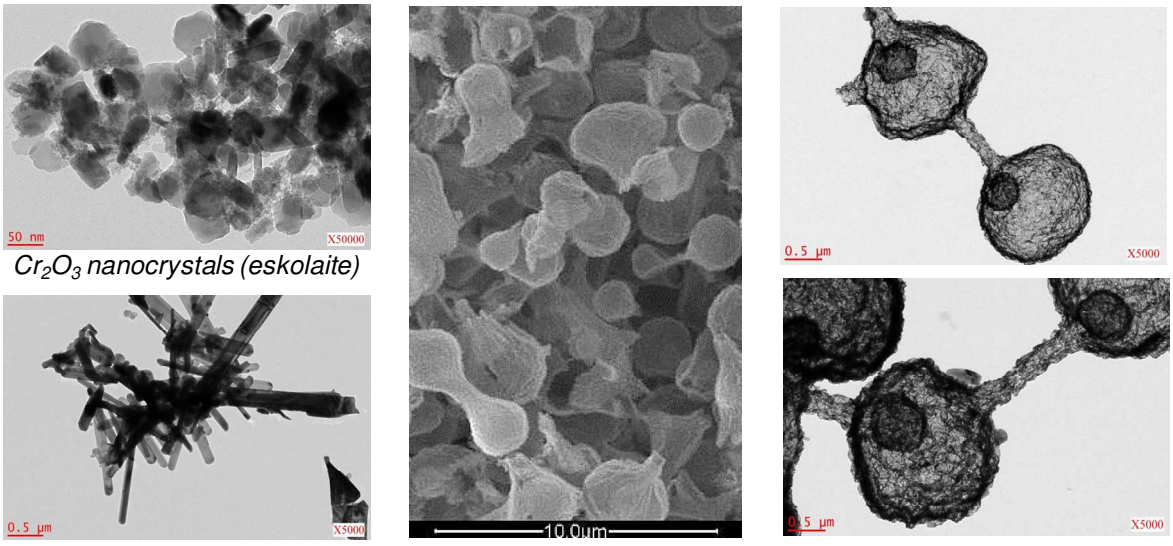

Cr_2O_3 nanocrystals (eskolaite)

V_2O_5 nanocrystals (shcherbinaite)

NiO hollow microspheres (bunsenite)

Fe_2O_3 hollow microspheres (hematite + β Fe_2O_3)

Figure 17. (a) Microspheres of tannin-based hydrothermal carbon, prepared in the same conditions (180°C, 24h) but in different aqueous solutions; (b) Ag-loaded, tannin-based carbon prepared in hydrothermal conditions in a solution of silver nitrate, followed by pyrolysis and slight oxidation to burn the carbon coating the Ag nanoparticles (top right), and selectivity towards ethylene epoxidation, compared to actual catalysts (bottom right); (c)

Mesoporous oxides obtained by calcination of tannin-based, metal-loaded hydrochars. (After [137] with permission from Elsevier, [138] with permission of Wiley, and [136] with permission from MDPI).

The strong ability of tannins to complex transition metals has been used to prepare either porous metal-carbon hybrids, or mesoporous metal oxides [136]. The former are easily prepared by treating tannins in hydrothermal conditions with an aqueous solution of metal salt, followed by pyrolysis: if the reduction potential of the metal is not too low, carbon at 900°C reduces the cations into metal nanoparticles dispersed in the carbon structure. This works well with Fe and Ni, for instance, and this is how tannin-based carbon can be partly graphitised, as already explained in section 2.1. But this also works with Ag, which can be subsequently used as catalyst deposited on a porous carbon support. Ag nanoparticles only need to be made available to the reactants through a soft oxidation, which burns the carbon layer coating them after synthesis. Then, the tannin-based, Ag-loaded porous carbon becomes an efficient catalyst for ethylene epoxidation, which is an important reaction since ethylene epoxide is involved in the synthesis of polyethylene glycol and is also used for medical disinfection, among other applications. Figure 17(b) shows that the catalytic performance of this material reasonably compares with those of actual industrial catalysts: what one loses in selectivity, one gains in yield, and vice versa [138].

Oxides are simply obtained by calcination in air of materials resulting from the hydrothermal treatment of tannin in metal salt solutions, unlike the former hybrid materials that had been pyrolysed. The dispersion state of the metal in the tannin-based polymer network promotes the spontaneous formation of mesoporous oxides. Figure 17(c) suggests that, at least for the examples given there, the metals from the left of the transitions series

(here V and Cr) lead to solid nano-crystals, whereas those of the right of the series (here Fe and Ni) lead to hollow microspheres whose shells are nanometre-thin.

At this point of this review on tannin-based carbons, one may wonder whether tannin pyrolysed directly at 900°C one the one hand, and tannin submitted to a preliminary hydrothermal carbonisation (HTC) and then subjected to the same pyrolysis conditions on the other hand, are the same materials. The answer is clearly no, although the differences between the two are not very large. WAXS and XPS studies indeed showed that both materials can be successfully modelled by a defective structure of bi-layer graphene of 375 atoms, i.e., by two slightly curved carbon layers distorted by defects and non-carbon atoms, having length and width of 2.05 nm and 1.75 nm, respectively (see Figure 18(a)). But the material having one HTC step in its preparation process is slightly more disordered, with 19% of mono-vacancies instead of 17% in tannin directly pyrolysed at 900°C (i.e., without HTC). It may also be added that, whereas both distributions of bond lengths are still centred on 1.42 Å, which corresponds to the graphitic structure, the distribution of the former carbon is broader due to more non-hexagonal carbon rings (see Figure 18(b)) [139]. This model does not mean that these structures of 375 atoms are the only ones or even exist, but they are a reasonable average of what represents the samples as a whole. Moreover, the above findings are in agreement with the Raman spectra that, despite their very similar and nearly superimposable aspects, show after deconvolution of their 1st order profiles that the intensity ratios of the bands D1 and G are definitely not the same. In the case of non-graphitisable carbon such as tannin pyrolysed in the absence of transition metals, a high D1/G ratio corresponds to a higher value of La, i.e., to more extended coherent domains. Besides, the FWHM of the G band is higher in the carbon with HTC, further supporting its more defective nature (Figure 18(c)). As final proof,

elemental analysis of the two kinds of carbons shows that HTC increased the contents of heteroelements, and thus slightly decreased the carbon level (see again Table 1).

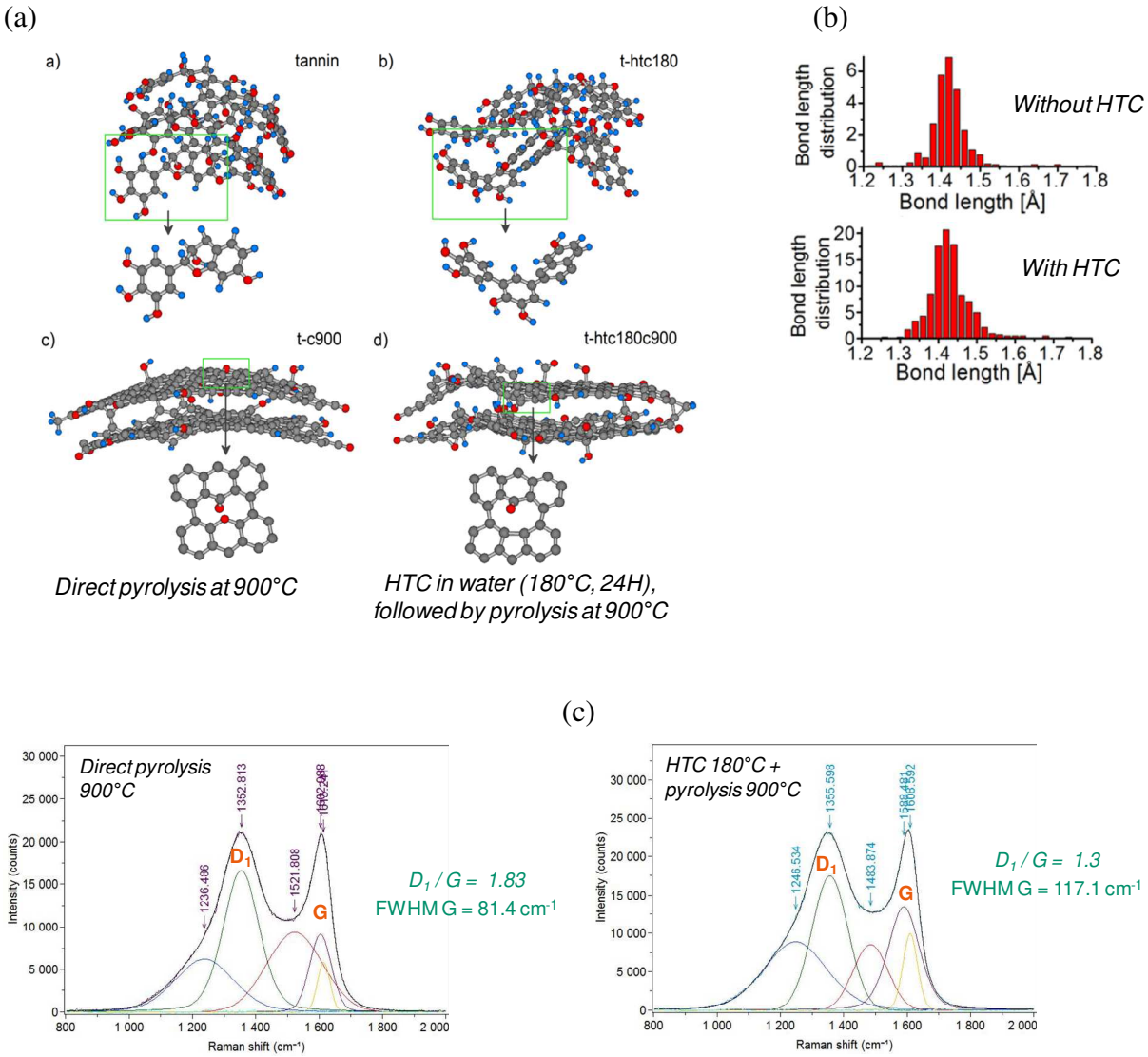

Figure 18. Differences between tannin-based carbons, whether directly pyrolysed at 900°C or submitted to hydrothermal carbonisation (HTC: 1h at 180°C) before pyrolysis at 900°C: (a) Model structures based on WAXS and XPS studies; (b) Corresponding bond length distributions; (c) Raman spectra. (Adapted from [139] with permission from the American Chemical Society).

These slight differences should not obscure the immense benefits of hydrothermal treatments as steps in the synthesis of carbon materials such as, as detailed above, the

possibility of depositing carbon onto various templates in mild conditions (i.e., an alternative to CVD in some cases), producing new structures and new materials (metal-carbon hybrids, mesoporous nano-oxides), and easily doping carbon with heteroelements (N, O, …) or loading it, more or less heavily, with metals (Fe, Ni, …), and hence possibly graphitising it.

6.2 Latest, new tannin-based carbons

It has also been highlighted above that tannin is a very relevant precursor of glassy carbon but, so far, the considered materials were either in divided form or in porous form. Obtaining solid glassy carbon from tannin-based viscous resins is also possible, by which various objects can be prepared (see Figure 19). The studies of the properties of this new material are presently in progress. The first results show that, as expected for this kind of carbon, the skeletal density decreases when the heat-treatment temperature increases from 800°C to 1600°C, and at the same time the oxygen content decreases whereas the size of the coherent domains (La) increases significantly. The material never graphitises, and undergoes no structural transition when compressed up to 30 GPa. Since its BET area is negligibly low, and because it is typically a hard carbon, it might be of interest for sodium-ion batteries. The corresponding tests are in progress.

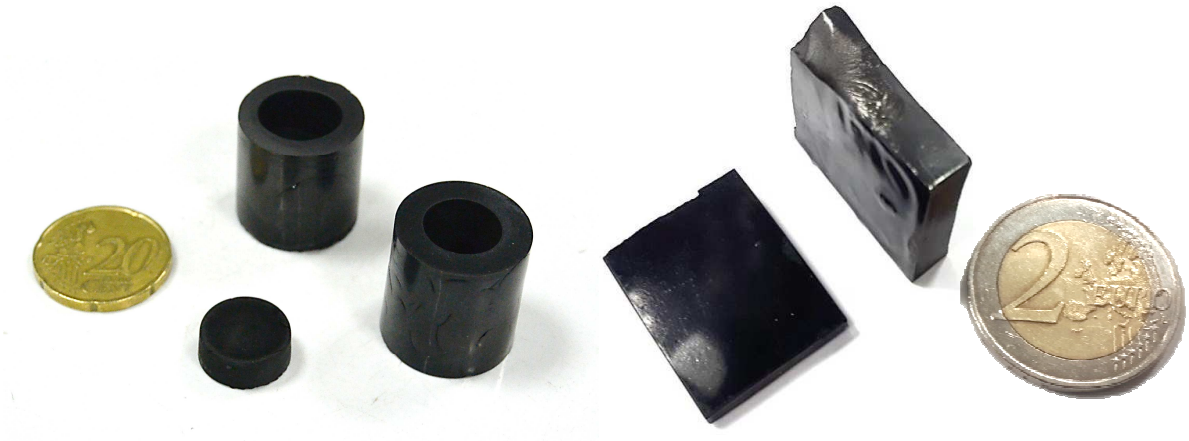

Figure 19. A few objects made of tannin-based glassy carbon.

Finally, the same kinds of tannin-based resins can be formed, as highlighted in the discussion of tannin-derived gels, in a very broad range of pH. Those prepared in acidic medium thus behave as novolacs, whereas those obtained in alkaline conditions have the properties of resoles. Therefore, industries presently handling such phenolic resins as precursors of various speciality carbons can certainly substitute part - or all - of them by tannins. We could successfully apply this concept to a few industrial processes, which became far greener without loss of performances. In fact, up to now, there is no example known to us where tannins have not been able to replace phenolic resins, whatever the applications. This statement applies to carbon precursors, until we find an example that demonstrates the opposite, which has never happened so far.

7. Conclusion

Tannins are natural polyphenolic molecules combining a number of unique benefits: bio-based, commercially available at low cost, reproducible, non-toxic but reactive. These precursors are the natural counterpart of resorcinol and phenol, from which many carbon aerogels have been described. Tannins can lead to the same materials with a cost about 5 times lower, while having many other advantages. Tannins are indeed much more versatile in the sense that they react with a number of crosslinkers over the entire pH range, and in different protic solvents. They can even polymerise without crosslinker by auto-condensation, thus leading to formaldehyde-free carbon precursors for example.

The exceptional richness of the formulations also allows producing thermoset resins of all morphologies, which, once polymerised, are insoluble and infusible and thus make it possible to obtain carbon materials of completely controlled structure. Thus, beyond gels, we

synthesised carbon foams but also ordered mesoporous carbons, porous carbon beads, hollow carbon spheres, carbon polyHIPEs, 3D periodic carbon structures and various kinds of glassy carbons. The solubility of tannins in water, coupled with their reactivity, also makes it possible to obtain nitrogen-doped carbons in one single step, anchor nanoparticles, or deposit hydrothermal carbon on various structures used as templates, whether hard or soft.

Also worth mentioning is the multitude of applications for which these tannin-derived carbons can be successfully used. Supercapacitor electrodes, carbon molecular sieves, platinum-free electrocatalysts for the oxygen reduction reaction in DMFC fuel cells, adsorption of CO_2, water / hydrocarbon separation, catalysis of ethylene epoxidation, UV photodegradation of dyes, encapsulation of phase change materials for seasonal heat storage, broadband absorption for microwave applications and sound absorption at controlled frequencies are worth quoting, amongst others. Finally, it should be noticed that tannin-derived carbons can be partly graphitised, and that the entire series of nanotextures from vitreous carbon to graphite-like through turbostratic carbon can be obtained. Therefore, not only the most diverse structures are possible by the proper structuring of precursor resins, but also once the carbons are obtained, the performances meet expectations, whether they deal with electrochemistry, adsorption, transport processes or responses to electromagnetic waves for example. This is explained by the control of the porosity by which any architecture is feasible from the same starting raw material on the one hand, but also by the possibility of adjusting the carbon texture on the other hand. As a result, a continuum of properties is accessible, from the isotropic to the highly anisotropic, from amorphous to graphite-like, from poorly to highly conductive. Moreover, the resulting carbon is reactive and therefore responds very well to doping and to surface functionalisation, further expanding its already broad possibilities of use.

For instance, 3D-printed structures and polymer capsules in aqueous solutions of tannin submitted to hydrothermal treatment and further pyrolysis yield periodic 3D carbon architectures and hollow carbon spheres, respectively. These materials behave like photonic crystals in the GHz-THz domain, and they were the first metamaterials for electromagnetic applications of this kind. The control of the structure of tannin resins-derived rigid foams also allowed, for the first time, to produce vitreous carbon foams of constant porosity but with variable cell size, or of variable porosity but with constant cell size. These unique features, associated with a strictly constant carbon composition and nanotexture, allowed studying with unequalled accuracy so far the influence of the porous structure of cellular materials on their mechanical, thermal, acoustic and electromagnetic properties. Tannin-based mesoporous carbons, either perfectly ordered or with a worm-like structure but presenting the same single mesopore size, are also now being tested for calibrating image reconstruction algorithms for electron tomography and for applying advanced adsorption models. Theoretical advances can thus be achieved by the realisation of model materials based on biosourced carbons.

These particularly fruitful works undeniably demonstrate that biomass can be the source of very fundamental works and of high-technology materials. These studies also plead for a massive use of bioresources as precursors of carbon materials, whose performances are not inferior to those of their synthetic counterparts, in a critical context of depletion of raw materials. There is indeed no example so far of carbon materials based on phenolic material that could not be realised from tannins, and this conclusion is of special interest for industries that use high temperatures in their processes and that require much greener resources. Many other examples might be given, confirming the potential of bio-based carbons for the extraordinary range of technological solutions they can offer. Other examples that have not been reported in this review are related to the possibility of producing carbon microfibers,

carbon dots, and taking advantage of the photo-sensibility of tannins to induce UV-triggered polymerisation and to produce new carbon materials.

In conclusion, polyphenolic plant extracts are definitely new precursors of interest for all kinds of functional carbons, the applications of which are directly functions of both porous structure and surface chemistry. In other words, tannins appear in light of these works as a new "Swiss Army Knife" in most – if not all – applications where porous carbons are needed.

Acknowledgements

The research leading to these results has received funding from the CPER 2007-2013 “Structuration du Pôle de Compétitivité Fibres Grand’Est” (Competitiveness Fibre Cluster), through local (Conseil Général des Vosges), regional (Région Lorraine), national (DRRT and FNADT) and European (FEDER) funds. The authors also gratefully acknowledge the financial support of European FEDER funds (TALiSMAN project, 2019-000214), and thank the many colleagues and PhD and post-doctoral students who participated to these works and whose names appear in the reference list.

References

[1] A. Bianco, Y. Chen, Y. Chen, D. Ghoshal, R.H. Hurt, Y.A. Kim, N. Koratkar, V. Meunier, M. Terrones, A carbon science perspective in 2018: Current achievements and future challenges, Carbon. 132 (2018) 785–801. https://doi.org/10.1016/j.carbon.2018.02.058.

[2] K. Muellen, X. Feng, Chemistry of Carbon Nanostructures, De Gruyter, Berlin, Boston, 2017. https://doi.org/10.1515/9783110284645.

[3] Z. Yang, J. Tian, Z. Yin, C. Cui, W. Qian, F. Wei, Carbon nanotube- and graphene-based nanomaterials and applications in high-voltage supercapacitor: A review, Carbon. 141 (2019) 467–480. https://doi.org/10.1016/j.carbon.2018.10.010.

[4] N.C. Gallego, J.W. Klett, Carbon foams for thermal management, Carbon. 41 (2003) 1461–1466. https://doi.org/10.1016/S0008-6223(03)00091-5.

[5] M. Wiener, G. Reichenauer, S. Braxmeier, F. Hemberger, H.-P. Ebert, Carbon Aerogel-Based High-Temperature Thermal Insulation, Int J Thermophys. 30 (2009) 1372–1385. https://doi.org/10.1007/s10765-009-0595-1.

[6] H. Ji, D.P. Sellan, M.T. Pettes, X. Kong, J. Ji, L. Shi, R.S. Ruoff, Enhanced thermal conductivity of phase change materials with ultrathin-graphite foams for thermal energy storage, Energy Environ. Sci. 7 (2014) 1185–1192. https://doi.org/10.1039/C3EE42573H.

[7] V. Canseco, Y. Anguy, J.J. Roa, E. Palomo, Structural and mechanical characterization of graphite foam/phase change material composites, Carbon. 74 (2014) 266–281. https://doi.org/10.1016/j.carbon.2014.03.031.

[8] Y. Zhong, S. Li, X. Wei, Z. Liu, Q. Guo, J. Shi, L. Liu, Heat transfer enhancement of paraffin wax using compressed expanded natural graphite for thermal energy storage, Carbon. 48 (2010) 300–304. https://doi.org/10.1016/j.carbon.2009.09.033.

[9] K. Lafdi, O. Mesalhy, A. Elgafy, Graphite foams infiltrated with phase change materials as alternative materials for space and terrestrial thermal energy storage applications, Carbon. 46 (2008) 159–168. https://doi.org/10.1016/j.carbon.2007.11.003.

[10] O. Mesalhy, K. Lafdi, A. Elgafy, Carbon foam matrices saturated with PCM for thermal protection purposes, Carbon. 44 (2006) 2080–2088. https://doi.org/10.1016/j.carbon.2005.12.019.

[11] I. Kholmanov, J. Kim, E. Ou, R.S. Ruoff, L. Shi, Continuous Carbon Nanotube–Ultrathin Graphite Hybrid Foams for Increased Thermal Conductivity and Suppressed Subcooling in Composite Phase Change Materials, ACS Nano. 9 (2015) 11699–11707. https://doi.org/10.1021/acsnano.5b02917.

[12] E. Kockrick, C. Schrage, L. Borchardt, N. Klein, M. Rose, I. Senkovska, S. Kaskel, Ordered mesoporous carbide derived carbons for high pressure gas storage, Carbon. 48 (2010) 1707–1717. https://doi.org/10.1016/j.carbon.2010.01.004.

[13] J. Liu, Y. Zhou, Y. Sun, W. Su, L. Zhou, Methane storage in wet carbon of tailored pore sizes, Carbon. 49 (2011) 3731–3736. https://doi.org/10.1016/j.carbon.2011.05.005.

[14] G. Sdanghi, V. Nicolas, K. Mozet, G. Maranzana, A. Celzard, V. Fierro, Modelling of a hydrogen thermally driven compressor based on cyclic adsorption-desorption on activated carbon, International Journal of Hydrogen Energy. 44 (2019) 16811–16823. https://doi.org/10.1016/j.ijhydene.2019.04.233.

[15] M. Jordá-Beneyto, F. Suárez-García, D. Lozano-Castelló, D. Cazorla-Amorós, A. Linares-Solano, Hydrogen storage on chemically activated carbons and carbon nanomaterials at high pressures, Carbon. 45 (2007) 293–303. https://doi.org/10.1016/j.carbon.2006.09.022.

[16] D. Li, J. Zhou, Z. Zhang, L. Li, Y. Tian, Y. Lu, Y. Qiao, J. Li, L. Wen, Improving low-pressure CO2 capture performance of N-doped active carbons by adjusting flow rate of protective gas during alkali activation, Carbon. 114 (2017) 496–503. https://doi.org/10.1016/j.carbon.2016.12.039.

[17] K. Kante, M. Florent, A. Temirgaliyeva, B. Lesbayev, T.J. Bandosz, Exploring resistance changes of porous carbon upon physical adsorption of VOCs, Carbon. 146 (2019) 568–571. https://doi.org/10.1016/j.carbon.2019.02.039.

[18] F. Blanco, X. Vilanova, V. Fierro, A. Celzard, P. Ivanov, E. Llobet, N. Cañellas, J.L. Ramírez, X. Correig, Fabrication and characterisation of microporous activated carbon-based pre-concentrators for benzene vapours, Sensors and Actuators B: Chemical. 132 (2008) 90–98. https://doi.org/10.1016/j.snb.2008.01.016.

[19] N.A. Travlou, T.J. Bandosz, N-doped polymeric resin-derived porous carbons as efficient ammonia removal and detection media, Carbon. 117 (2017) 228–239. https://doi.org/10.1016/j.carbon.2017.02.099.

[20] D. Jiang, V.R. Cooper, S. Dai, Porous Graphene as the Ultimate Membrane for Gas Separation, Nano Lett. 9 (2009) 4019–4024. https://doi.org/10.1021/nl9021946.

[21] M. Seredych, D. Hulicova-Jurcakova, G.Q. Lu, T.J. Bandosz, Surface functional groups of carbons and the effects of their chemical character, density and accessibility to ions on electrochemical performance, Carbon. 46 (2008) 1475–1488. https://doi.org/10.1016/j.carbon.2008.06.027.

[22] C. Merlet, B. Rotenberg, P.A. Madden, P.-L. Taberna, P. Simon, Y. Gogotsi, M. Salanne, On the molecular origin of supercapacitance in nanoporous carbon electrodes, Nature Mater. 11 (2012) 306–310. https://doi.org/10.1038/nmat3260.

[23] Y. Shao, J. Xiao, W. Wang, M. Engelhard, X. Chen, Z. Nie, M. Gu, L.V. Saraf, G. Exarhos, J.-G. Zhang, J. Liu, Surface-Driven Sodium Ion Energy Storage in Nanocellular Carbon Foams, Nano Lett. 13 (2013) 3909–3914. https://doi.org/10.1021/nl401995a.

[24] C. Bommier, W. Luo, W.-Y. Gao, A. Greaney, S. Ma, X. Ji, Predicting capacity of hard carbon anodes in sodium-ion batteries using porosity measurements, Carbon. 76 (2014) 165–174. https://doi.org/10.1016/j.carbon.2014.04.064.

[25] J. Tang, J. Liu, N.L. Torad, T. Kimura, Y. Yamauchi, Tailored design of functional nanoporous carbon materials toward fuel cell applications, Nano Today. 9 (2014) 305–323. https://doi.org/10.1016/j.nantod.2014.05.003.

[26] J.B. Goodenough, A. Hamnett, B.J. Kennedy, R. Manoharan, S.A. Weeks, Porous carbon anodes for the direct methanol fuel cell—I. The role of the reduction method for

carbon supported platinum electrodes, Electrochimica Acta. 35 (1990) 199–207. https://doi.org/10.1016/0013-4686(90)85059-V.

[27] Y. Yang, K. Chiang, N. Burke, Porous carbon-supported catalysts for energy and environmental applications: A short review, Catalysis Today. 178 (2011) 197–205. https://doi.org/10.1016/j.cattod.2011.08.028.

[28] P. Serp, B. Machado, Nanostructured Carbon Materials for Catalysis, Royal Society of Chemistry, 2015. https://doi.org/10.1039/9781782622567.

[29] T.J. Bandosz, C.O. Ania, Origin and Perspectives of the Photochemical Activity of Nanoporous Carbons, Advanced Science. 5 (2018) 1800293. https://doi.org/10.1002/advs.201800293.

[30] T.J. Bandosz, A. Policicchio, M. Florent, W. Li, P.S. Poon, J. Matos, Solar light-driven photocatalytic degradation of phenol on S-doped nanoporous carbons: The role of functional groups in governing activity and selectivity, Carbon. 156 (2020) 10–23. https://doi.org/10.1016/j.carbon.2019.09.037.

[31] W. Li, B. Herkt, M. Seredych, T.J. Bandosz, Pyridinic-N groups and ultramicropore nanoreactors enhance CO2 electrochemical reduction on porous carbon catalysts, Applied Catalysis B: Environmental. 207 (2017) 195–206. https://doi.org/10.1016/j.apcatb.2017.02.023.

[32] Novel Carbon Adsorbents - 1st Edition, Elsevier, J.M.D. Tascon, 2012. https://www.elsevier.com/books/novel-carbon-adsorbents/tascon/978-0-08-097744-7.

[33] E.M. Carter, L.E. Katz, G.E. Speitel, D. Ramirez, Gas-Phase Formaldehyde Adsorption Isotherm Studies on Activated Carbon: Correlations of Adsorption Capacity to Surface Functional Group Density, Environ. Sci. Technol. 45 (2011) 6498–6503. https://doi.org/10.1021/es104286d.

[34] L. Wang, L. Rao, B. Xia, L. Wang, L. Yue, Y. Liang, H. DaCosta, X. Hu, Highly efficient CO2 adsorption by nitrogen-doped porous carbons synthesized with low-temperature sodium amide activation, Carbon. 130 (2018) 31–40. https://doi.org/10.1016/j.carbon.2018.01.003.

[35] N.A. Eltekova, D. Berek, I. Novák, F. Belliardo, Adsorption of organic compounds on porous carbon sorbents, Carbon. 38 (2000) 373–377. https://doi.org/10.1016/S0008-6223(99)00113-X.

[36] R.-L. Tseng, F.-C. Wu, R.-S. Juang, Liquid-phase adsorption of dyes and phenols using pinewood-based activated carbons, Carbon. 41 (2003) 487–495. https://doi.org/10.1016/S0008-6223(02)00367-6.

[37] M.J. Ahmed, Adsorption of quinolone, tetracycline, and penicillin antibiotics from aqueous solution using activated carbons: Review, Environmental Toxicology and Pharmacology. 50 (2017) 1–10. https://doi.org/10.1016/j.etap.2017.01.004.

[38] F. Mansour, M. Al-Hindi, R. Yahfoufi, G.M. Ayoub, M.N. Ahmad, The use of activated carbon for the removal of pharmaceuticals from aqueous solutions: a review, Rev Environ Sci Biotechnol. 17 (2018) 109–145. https://doi.org/10.1007/s11157-017-9456-8.

[39] M. Rafatullah, O. Sulaiman, R. Hashim, A. Ahmad, Adsorption of methylene blue on low-cost adsorbents: A review, Journal of Hazardous Materials. 177 (2010) 70–80. https://doi.org/10.1016/j.jhazmat.2009.12.047.

[40] J.M. Dias, M.C.M. Alvim-Ferraz, M.F. Almeida, J. Rivera-Utrilla, M. Sánchez-Polo, Waste materials for activated carbon preparation and its use in aqueous-phase treatment: A review, Journal of Environmental Management. 85 (2007) 833–846. https://doi.org/10.1016/j.jenvman.2007.07.031.

[41] W.-L. Song, M.-S. Cao, L.-Z. Fan, M.-M. Lu, Y. Li, C.-Y. Wang, H.-F. Ju, Highly ordered porous carbon/wax composites for effective electromagnetic attenuation and shielding, Carbon. 77 (2014) 130–142. https://doi.org/10.1016/j.carbon.2014.05.014.

[42] Q. Liu, J. Gu, W. Zhang, Y. Miyamoto, Z. Chen, D. Zhang, Biomorphic porous graphitic carbon for electromagnetic interference shielding, J. Mater. Chem. 22 (2012) 21183–21188. https://doi.org/10.1039/C2JM34590K.

[43] F. Moglie, D. Micheli, S. Laurenzi, M. Marchetti, V. Mariani Primiani, Electromagnetic shielding performance of carbon foams, Carbon. 50 (2012) 1972–1980. https://doi.org/10.1016/j.carbon.2011.12.053.

[44] Z. Zeng, Y. Zhang, X.Y.D. Ma, S.I.S. Shahabadi, B. Che, P. Wang, X. Lu, Biomass-based honeycomb-like architectures for preparation of robust carbon foams with high electromagnetic interference shielding performance, Carbon. 140 (2018) 227–236. https://doi.org/10.1016/j.carbon.2018.08.061.

[45] L.-L. Yang, C.-C. Wang, K.-Y. Yen, T. Yoshida, T. Hatano, T. Okuda, Antitumor Activities of Ellagitannins on Tumor Cell Lines, in: G.G. Gross, R.W. Hemingway, T. Yoshida (Eds.), Plant Polyphenols 2: Chemistry, Biology, Pharmacology, Ecology, Springer US, 1999: pp. 615–628. https://doi.org/10.1007/978-1-4615-4139-4.

[46] Y. Kashiwada, G. Nonaka, I. Nishioka, J.-J. Chang, K.-H. Lee, Antitumor Agents, 129. Tannins and Related Compounds as Selective Cytotoxic Agents, J. Nat. Prod. 55 (1992) 1033–1043. https://doi.org/10.1021/np50086a002.

[47] K. Funatogawa, S. Hayashi, H. Shimomura, T. Yoshida, T. Hatano, H. Ito, Y. Hirai, Antibacterial Activity of Hydrolyzable Tannins Derived from Medicinal Plants against Helicobacter pylori, Microbiology and Immunology. 48 (2004) 251–261. https://doi.org/10.1111/j.1348-0421.2004.tb03521.x.

[48] S. Quideau, M. Jourdes, C. Saucier, Y. Glories, P. Pardon, C. Baudry, DNA Topoisomerase Inhibitor Acutissimin A and Other Flavano-Ellagitannins in Red Wine, Angewandte Chemie International Edition. 42 (2003) 6012–6014. https://doi.org/10.1002/anie.200352089.

[49] A. Ricci, G.P. Parpinello, A.S. Palma, N. Teslić, C. Brilli, A. Pizzi, A. Versari, Analytical profiling of food-grade extracts from grape (Vitis vinifera sp.) seeds and skins, green tea (Camellia sinensis) leaves and Limousin oak (Quercus robur) heartwood using MALDI-TOF-MS, ICP-MS and spectrophotometric methods, Journal of Food Composition and Analysis. 59 (2017) 95–104. https://doi.org/10.1016/j.jfca.2017.01.014.

[50] C.T. Robbins, S. Mole, A.E. Hagerman, T.A. Hanley, Role of Tannins in Defending Plants Against Ruminants: Reduction in Dry Matter Digestion?, Ecology. 68 (1987) 1606–1615. https://doi.org/10.2307/1939852.

[51] S.J. Cork, A.K. Krockenberger, Methods and pitfalls of extracting condensed tannins and other phenolics from plants: Insights from investigations onEucalyptus leaves, Journal of Chemical Ecology. 17 (1991) 123–134. https://doi.org/10.1007/BF00994426.

[52] H.P.S. Makkar, K. Becker, Isolation of Tannins from Leaves of Some Trees and Shrubs and Their Properties, J. Agric. Food Chem. 42 (1994) 731–734. https://doi.org/10.1021/jf00039a026.

[53] A. Scalbert, B. Monties, G. Janin, Tannins in wood: comparison of different estimation methods, J. Agric. Food Chem. 37 (1989) 1324–1329. https://doi.org/10.1021/jf00089a026.

[54] E. Haslam, Plant Polyphenols: Vegetable Tannins Revisited, Cambridge University Press, New York, 1989.

[55] A. Pizzi, Chapter 8 - Tannins: Major Sources, Properties and Applications, in: M.N. Belgacem, A. Gandini (Eds.), Monomers, Polymers and Composites from Renewable Resources, Elsevier, Amsterdam, 2008: pp. 179–199. https://doi.org/10.1016/B978-0-08-045316-3.00008-9.

[56] A. Arenillas, J.A. Menéndez, G. Reichenauer, A. Celzard, V. Fierro, F.J.M. Hodar, E. Bailón-Garcia, N. Job, Organic and Carbon Gels Derived from Biosourced Polyphenols, in: Organic and Carbon Gels: From Laboratory Synthesis to Applications, Springer International Publishing, 2019: pp. 27–86. https://doi.org/10.1007/978-3-030-13897-4.

[57] C. Aouf, S. Benyahya, A. Esnouf, S. Caillol, B. Boutevin, H. Fulcrand, Tara tannins as phenolic precursors of thermosetting epoxy resins, European Polymer Journal. 55 (2014) 186–198. https://doi.org/10.1016/j.eurpolymj.2014.03.034.

[58] K.M. Nelson, S.M. Mahurin, R.T. Mayes, B. Williamson, C.M. Teague, A.J. Binder, L. Baggetto, G.M. Veith, S. Dai, Preparation and CO2 adsorption properties of soft-templated mesoporous carbons derived from chestnut tannin precursors, Microporous and Mesoporous Materials. 222 (2016) 94–103. https://doi.org/10.1016/j.micromeso.2015.09.050.

[59] A. Pizzi, Tannins: Prospectives and Actual Industrial Applications, Biomolecules. 9 (2019) 344. https://doi.org/10.3390/biom9080344.

[60] V. Fierro, jimena Castro-Gutierrez, A. Celzard, Tannins as new, green, precursors of mesoporous carbons, in: Proceedings of the International Conference Woodchem 2019, Nancy (France), 2019.

[61] V. Fierro, J.E. Monsivais-Rocha, A. Celzard, Synthesis of mesoporous carbons from hydrolysable tannins without aldehydes, in: Proceedings of the International Conference Carbon 2019, Lexington, KY (USA), 2019.

[62] P. Luckeneder, J. Gavino, R. Kuchernig, A. Petutschnigg, G. Tondi, Sustainable Phenolic Fractions as Basis for Furfuryl Alcohol-Based Co-Polymers and Their Use as Wood Adhesives, Polymers. 8 (2016) 396. https://doi.org/10.3390/polym8110396.

[63] X. Li, A. Nicollin, A. Pizzi, X. Zhou, A. Sauget, L. Delmotte, Natural tannin–furanic thermosetting moulding plastics, RSC Adv. 3 (2013) 17732–17740. https://doi.org/10.1039/C3RA43095B.

[64] N. Meikleham, A. Pizzi, A. Stephanou, Induced accelerated autocondensation of polyflavonoid tannins for phenolic polycondensates. I. 13C-NMR, 29Si-NMR, X-ray, and polarimetry studies and mechanism, Journal of Applied Polymer Science. 54 (1994) 1827–1845. https://doi.org/10.1002/app.1994.070541206.

[65] A. Pizzi, N. Meikleham, Induced accelerated autocondensation of polyflavonoid tannins for phenolic polycondensates. III. CP-MAS 13C-NMR of different tannins and models, Journal of Applied Polymer Science. 55 (1995) 1265–1269. https://doi.org/10.1002/app.1995.070550812.

[66] X. Li, M.C. Basso, F.L. Braghiroli, V. Fierro, A. Pizzi, A. Celzard, Tailoring the structure of cellular vitreous carbon foams, Carbon. 50 (2012) 2026–2036. https://doi.org/10.1016/j.carbon.2012.01.004.

[67] G. Tondi, V. Fierro, A. Pizzi, A. Celzard, Tannin-based carbon foams, Carbon. 47 (2009) 1480–1492. https://doi.org/10.1016/j.carbon.2009.01.041.

[68] W. Zhao, A. Pizzi, V. Fierro, G. Du, A. Celzard, Effect of composition and processing parameters on the characteristics of tannin-based rigid foams. Part I: Cell structure, Materials Chemistry and Physics. 122 (2010) 175–182. https://doi.org/10.1016/j.matchemphys.2010.02.062.

[69] A. Szczurek, V. Fierro, A. Pizzi, M. Stauber, A. Celzard, Carbon meringues derived from flavonoid tannins, Carbon. 65 (2013) 214–227. https://doi.org/10.1016/j.carbon.2013.08.017.

[70] L.I. Grishechko, G. Amaral-Labat, V. Fierro, A. Szczurek, B.N. Kuznetsov, A. Celzard, Biosourced, highly porous, carbon xerogel microspheres, RSC Adv. 6 (2016) 65698–65708. https://doi.org/10.1039/C6RA09462G.

[71] A. Szczurek, G. Amaral-Labat, V. Fierro, A. Pizzi, E. Masson, A. Celzard, The use of tannin to prepare carbon gels. Part I: Carbon aerogels, Carbon. 49 (2011) 2773–2784. https://doi.org/10.1016/j.carbon.2011.03.007.

[72] G. Amaral-Labat, A. Szczurek, V. Fierro, A. Celzard, Unique bimodal carbon xerogels from soft templating of tannin, Materials Chemistry and Physics. 149–150 (2015) 193–201. https://doi.org/10.1016/j.matchemphys.2014.10.006.

[73] A. Szczurek, V. Fierro, A. Plyushch, J. Macutkevic, P. Kuzhir, A. Celzard, Structure and Electromagnetic Properties of Cellular Glassy Carbon Monoliths with Controlled Cell Size, Materials. 11 (2018) 709–1 – 709–19. https://doi.org/10.3390/ma11050709.

[74] P. Jana, V. Fierro, A. Pizzi, A. Celzard, Thermal conductivity improvement of composite carbon foams based on tannin-based disordered carbon matrix and graphite fillers, Materials & Design. 83 (2015) 635–643. https://doi.org/10.1016/j.matdes.2015.06.057.

[75] M. Letellier, A. Szczurek, M.-C. Basso, A. Pizzi, V. Fierro, O. Ferry, A. Celzard, Preparation and structural characterisation of model cellular vitreous carbon foams, Carbon. 112 (2017) 208–218. https://doi.org/10.1016/j.carbon.2016.11.017.

[76] Y.S. Touloukian, R.K. Kirby, Thermal expansion--nonmetallic solids, IFI/Plenum, New York, 1977.

[77] M. Letellier, Optimisation de mousses de carbone dérivées de tannin par l'étude et la modélisation de leurs propriétés physiques, Université de Lorraine, 2015. https://www.theses.fr/2015LORR0165.

[78] A. Pizzi, ed., Tannin-based wood adhesives, in: Wood Adhesives: Chemistry and Technology, 1 edition, CRC Press, New York, 1983: pp. 177–246.

[79] J. Jagiello, J. Kenvin, A. Celzard, V. Fierro, Enhanced resolution of ultra micropore size determination of biochars and activated carbons by dual gas analysis using N2 and CO2 with 2D-NLDFT adsorption models, Carbon. 144 (2019) 206–215. https://doi.org/10.1016/j.carbon.2018.12.028.

[80] G. Tondi, A. Pizzi, H. Pasch, A. Celzard, Structure degradation, conservation and rearrangement in the carbonisation of polyflavonoid tannin/furanic rigid foams – A MALDI-TOF investigation, Polymer Degradation and Stability. 93 (2008) 968–975. https://doi.org/10.1016/j.polymdegradstab.2008.01.024.

[81] G. Tondi, A. Pizzi, H. Pasch, A. Celzard, K. Rode, MALDI-ToF investigation of furanic polymer foams before and after carbonization: Aromatic rearrangement and surviving furanic structures, European Polymer Journal. 44 (2008) 2938–2943. https://doi.org/10.1016/j.eurpolymj.2008.06.029.

[82] M. Letellier, C. Delgado-Sanchez, M. Khelifa, V. Fierro, A. Celzard, Mechanical properties of model vitreous carbon foams, Carbon. 116 (2017) 562–571. https://doi.org/10.1016/j.carbon.2017.02.020.

[83] M. Letellier, S. Ghaffari Mosanenzadeh, H. Naguib, V. Fierro, A. Celzard, Acoustic properties of model cellular vitreous carbon foams, Carbon. 119 (2017) 241–250. https://doi.org/10.1016/j.carbon.2017.04.049.

[84] G. Amaral-Labat, E. Gourdon, V. Fierro, A. Pizzi, A. Celzard, Acoustic properties of cellular vitreous carbon foams, Carbon. 58 (2013) 76–86. https://doi.org/10.1016/j.carbon.2013.02.033.

[85] A. Celzard, V. Nicolas, M. Letellier, V. Fierro, Thermal conductivity of model cellular vitreous carbon foams, in: Proceedings of the International Conference Carbon 2019, Lexington, KY (USA), 2019.

[86] A. Celzard, G. Tondi, D. Lacroix, G. Jeandel, B. Monod, V. Fierro, A. Pizzi, Radiative properties of tannin-based, glasslike, carbon foams, Carbon. 50 (2012) 4102–4113. https://doi.org/10.1016/j.carbon.2012.04.058.

[87] M. Letellier, J. Macutkevic, P. Kuzhir, J. Banys, V. Fierro, A. Celzard, Electromagnetic properties of model vitreous carbon foams, Carbon. 122 (2017) 217–227. https://doi.org/10.1016/j.carbon.2017.06.080.

[88] M. Letellier, J. Macutkevic, A. Paddubskaya, A. Plyushch, P. Kuzhir, M. Ivanov, J. Banys, A. Pizzi, V. Fierro, A. Celzard, Tannin-based carbon foams for electromagnetic applications, IEEE Transactions on Electromagnetic Compatibility. 57 (2015) 989–995. https://doi.org/10.1109/TEMC.2015.2430370.

[89] W. Zhao, V. Fierro, A. Pizzi, G. Du, A. Celzard, Effect of composition and processing parameters on the characteristics of tannin-based rigid foams. Part II: Physical properties, Materials Chemistry and Physics. 123 (2010) 210–217. https://doi.org/10.1016/j.matchemphys.2010.03.084.

[90] X. Li, V.K. Srivastava, A. Pizzi, A. Celzard, J. Leban, Nanotube-reinforced tannin/furanic rigid foams, Industrial Crops and Products. 43 (2013) 636–639. https://doi.org/10.1016/j.indcrop.2012.08.008.

[91] P. Jana, V. Fierro, A. Pizzi, A. Celzard, Biomass-derived, thermally conducting, carbon foams for seasonal thermal storage, Biomass and Bioenergy. 67 (2014) 312–318. https://doi.org/10.1016/j.biombioe.2014.04.031.

[92] P. Jana, E. Palomo del Barrio, V. Fierro, G. Medjahdi, A. Celzard, Design of carbon foams for seasonal solar thermal energy storage, Carbon. 109 (2016) 771–787. https://doi.org/10.1016/j.carbon.2016.08.048.

[93] A. Szczurek, V. Fierro, A. Pizzi, A. Celzard, Mayonnaise, whipped cream and meringue, a new carbon cuisine, Carbon. 58 (2013) 245–248. https://doi.org/10.1016/j.carbon.2013.02.056.

[94] A. Szczurek, V. Fierro, A. Pizzi, A. Celzard, Emulsion-templated porous carbon monoliths derived from tannins, Carbon. 74 (2014) 352–362. https://doi.org/10.1016/j.carbon.2014.03.047.

[95] M. Seredych, A. Szczurek, V. Fierro, A. Celzard, T.J. Bandosz, Electrochemical reduction of oxygen on hydrophobic ultramicroporous polyHIPE carbon, ACS Catal. 6 (2016) 5618–5628. https://doi.org/10.1021/acscatal.6b01497.

[96] A. Szczurek, V. Fierro, A. Pizzi, M. Stauber, A. Celzard, A new method for preparing tannin-based foams, Industrial Crops and Products. 54 (2014) 40–53. https://doi.org/10.1016/j.indcrop.2014.01.012.

[97] J. Encalada, K. Savaram, N.A. Travlou, W. Li, Q. Li, C. Delgado-Sánchez, V. Fierro, A. Celzard, H. He, T.J. Bandosz, Combined effect of porosity and surface chemistry on the electrochemical reduction of oxygen on cellular vitreous carbon foam catalyst, ACS Catal. 7 (2017) 7466–7478. https://doi.org/10.1021/acscatal.7b01977.

[98] A. Szczurek, A. Ortona, L. Ferrari, E. Rezaei, G. Medjahdi, V. Fierro, D. Bychanok, P. Kuzhir, A. Celzard, Carbon periodic cellular architectures, Carbon. 88 (2015) 70–85. https://doi.org/10.1016/j.carbon.2015.02.069.

[99] D. Bychanok, A. Paddubskaya, P. Kuzhir, A. Ortona, E. Rezaei, V. Fierro, A. Celzard, Carbon photonic crystals for electromagnetic applications, in: Proceedings of the International Conference Carbon 2016, State College, PA (USA), 2016.

[100] D. Bychanok, S. Li, A. Sanchez-Sanchez, G. Gorokhov, P. Kuzhir, F.Y. Ogrin, A. Pasc, T. Ballweg, K. Mandel, A. Szczurek, V. Fierro, A. Celzard, Hollow carbon spheres in microwaves: Bio inspired absorbing coating, Appl. Phys. Lett. 108 (2016) 013701-1 – 013701-5. https://doi.org/10.1063/1.4938537.

[101] S. Li, A. Celzard, V. Fierro, A. Pasc, Salting Effect in the Hydrothermal Carbonisation of Bioresources, ChemistrySelect. 1 (2016) 4161–4166. https://doi.org/10.1002/slct.201600837.

[102] A. Celzard, A. Pasc, S. Schaefer, K. Mandel, T. Ballweg, S. Li, G. Medjahdi, V. Nicolas, V. Fierro, Floating hollow carbon spheres for improved solar evaporation, Carbon. 146 (2019) 232–247. https://doi.org/10.1016/j.carbon.2019.01.101.

[103] A.-H. Lu, F. Schüth, Nanocasting: A Versatile Strategy for Creating Nanostructured Porous Materials, Advanced Materials. 18 (2006) 1793–1805. https://doi.org/10.1002/adma.200600148.

[104] T. Kyotani, Control of pore structure in carbon, Carbon. 38 (2000) 269–286. https://doi.org/10.1016/S0008-6223(99)00142-6.

[105] S. Jun, S.H. Joo, R. Ryoo, M. Kruk, M. Jaroniec, Z. Liu, T. Ohsuna, O. Terasaki, Synthesis of New, Nanoporous Carbon with Hexagonally Ordered Mesostructure, J. Am. Chem. Soc. 122 (2000) 10712–10713. https://doi.org/10.1021/ja002261e.

[106] K. Wu, Q. Liu, Nitrogen-doped mesoporous carbons for high performance supercapacitors, Applied Surface Science. 379 (2016) 132–139. https://doi.org/10.1016/j.apsusc.2016.04.064.

[107] M. Kruk, M. Jaroniec, R. Ryoo, S.H. Joo, Characterization of Ordered Mesoporous Carbons Synthesized Using MCM-48 Silicas as Templates, J. Phys. Chem. B. 104 (2000) 7960–7968. https://doi.org/10.1021/jp000861u.

[108] A. Sánchez-Sánchez, M.T. Izquierdo, J. Ghanbaja, G. Medjahdi, S. Mathieu, A. Celzard, V. Fierro, Excellent electrochemical performances of nanocast ordered mesoporous carbons based on tannin-related polyphenols as supercapacitor electrodes, Journal of Power Sources. 344 (2017) 15–24. https://doi.org/10.1016/j.jpowsour.2017.01.099.

[109] L. Chuenchom, R. Kraehnert, B.M. Smarsly, Recent progress in soft-templating of porous carbon materials, Soft Matter. 8 (2012) 10801–10812. https://doi.org/10.1039/C2SM07448F.

[110] P. Zhang, J. Zhang, S. Dai, Mesoporous Carbon Materials with Functional Compositions, Chemistry – A European Journal. 23 (2017) 1986–1998. https://doi.org/10.1002/chem.201602199.

[111] T. Liu, G. Liu, Block copolymer-based porous carbons for supercapacitors, J. Mater. Chem. A. 7 (2019) 23476–23488. https://doi.org/10.1039/C9TA07770G.

[112] D. Hou, J. Zhang, H. Tian, Q. Li, C. Li, Y. Mai, Pore Engineering of 2D Mesoporous Nitrogen-Doped Carbon on Graphene through Block Copolymer Self-Assembly, Advanced Materials Interfaces. 6 (2019) 1901476. https://doi.org/10.1002/admi.201901476.

[113] C. Liang, K. Hong, G.A. Guiochon, J.W. Mays, S. Dai, Synthesis of a Large-Scale Highly Ordered Porous Carbon Film by Self-Assembly of Block Copolymers, Angewandte Chemie International Edition. 43 (2004) 5785–5789. https://doi.org/10.1002/anie.200461051.

[114] S. Schlienger, A.-L. Graff, A. Celzard, J. Parmentier, Direct synthesis of ordered mesoporous polymer and carbon materials by a biosourced precursor, Green Chem. 14 (2012) 313–316. https://doi.org/10.1039/C2GC16160E.

[115] F.L. Braghiroli, V. Fierro, J. Parmentier, A. Pasc, A. Celzard, Easy and eco-friendly synthesis of ordered mesoporous carbons by self-assembly of tannin with a block copolymer, Green Chem. 18 (2016) 3265–3271. https://doi.org/10.1039/C5GC02788H.

[116] A. Sanchez-Sanchez, M.T. Izquierdo, G. Medjahdi, J. Ghanbaja, A. Celzard, V. Fierro, Ordered mesoporous carbons obtained by soft-templating of tannin in mild conditions, Microporous and Mesoporous Materials. 270 (2018) 127–139. https://doi.org/10.1016/j.micromeso.2018.05.017.

[117] J. Matos, P.S. Poon, V. Fierro, A. Sanchez-Sanchez, A. Celzard, Photocatalytic activity of semiconductor-free, tannin-derived mesostructured carbons, , in: Proceedings of the 8th International Conference on Carbon for Energy Storage and Environment Protection CESEP'19, Alicante (Spain), 2019.

[118] J. Castro-Gutiérrez, A. Sanchez-Sanchez, J. Ghanbaja, N. Díez, M. Sevilla, A. Celzard, V. Fierro, Synthesis of perfectly ordered mesoporous carbons by water-assisted mechanochemical self-assembly of tannin, Green Chem. 20 (2018) 5123–5132. https://doi.org/10.1039/C8GC02295J.

[119] E. García-Díez, S. Schaefer, A. Sanchez-Sanchez, A. Celzard, V. Fierro, M.M. Maroto-Valer, S. García, Novel Porous Carbons Derived from Coal Tar Rejects: Assessment of the Role of Pore Texture in CO2 Capture under Realistic Postcombustion Operating Temperatures, ACS Appl. Mater. Interfaces. 11 (2019) 36789–36799. https://doi.org/10.1021/acsami.9b13247.

[120] J. Castro-Gutiérrez, N. Díez, M. Sevilla, M.T. Izquierdo, J. Ghanbaja, A. Celzard, V. Fierro, High-Rate Capability of Supercapacitors Based on Tannin-Derived Ordered Mesoporous Carbons, ACS Sustainable Chem. Eng. 7 (2019) 17627–17635. https://doi.org/10.1021/acssuschemeng.9b03407.

[121] A. Szczurek, G. Amaral-Labat, V. Fierro, A. Pizzi, A. Celzard, The use of tannin to prepare carbon gels. Part II. Carbon cryogels, Carbon. 49 (2011) 2785–2794. https://doi.org/10.1016/j.carbon.2011.03.005.

[122] A. Pizzi, H. Pasch, A. Celzard, A. Szczurek, Oligomer distribution at the gel point of tannin-resorcinol-formaldehyde cold-set wood adhesives, Journal of Adhesion Science and Technology. 26 (2012) 79–88. https://doi.org/10.1163/016942411X569309.

[123] A. Pizzi, H. Pasch, A. Celzard, A. Szczurek, Oligomers distribution at the gel point of tannin–formaldehyde thermosetting adhesives for wood panels, Journal of Adhesion Science and Technology. 27 (2013) 2094–2102. https://doi.org/10.1080/01694243.2012.697669.

[124] G. Amaral-Labat, A. Szczurek, V. Fierro, A. Pizzi, A. Celzard, Systematic studies of tannin–formaldehyde aerogels: preparation and properties, Sci. Technol. Adv. Mater. 14 (2013) 015001. https://doi.org/10.1088/1468-6996/14/1/015001.

[125] L.I. Grishechko, G. Amaral-Labat, A. Szczurek, V. Fierro, B.N. Kuznetsov, A. Pizzi, A. Celzard, New tannin–lignin aerogels, Industrial Crops and Products. 41 (2013) 347–355. https://doi.org/10.1016/j.indcrop.2012.04.052.

[126] G. Amaral-Labat, L. Grishechko, A. Szczurek, V. Fierro, A. Pizzi, B. Kuznetsov, A. Celzard, Highly mesoporous organic aerogels derived from soy and tannin, Green Chem. 14 (2012) 3099–3106. https://doi.org/10.1039/C2GC36263E.

[127] G. Amaral-Labat, L.I. Grishechko, V. Fierro, B.N. Kuznetsov, A. Pizzi, A. Celzard, Tannin-based xerogels with distinctive porous structures, Biomass and Bioenergy. 56 (2013) 437–445. https://doi.org/10.1016/j.biombioe.2013.06.001.

[128] A. Szczurek, G. Amaral-Labat, V. Fierro, A. Pizzi, A. Celzard, Chemical activation of tannin-based hydrogels by soaking in KOH and NaOH solutions, Microporous and Mesoporous Materials. 196 (2014) 8–17. https://doi.org/10.1016/j.micromeso.2014.04.051.

[129] A. Szczurek, V. Fierro, G. Medjahdi, A. Celzard, Carbon aerogels prepared by autocondensation of flavonoid tannin, Carbon Resources Conversion. 2 (2019) 72–84. https://doi.org/10.1016/j.crcon.2019.02.001.

[130] F. Braghiroli, V. Fierro, A. Pizzi, K. Rode, W. Radke, L. Delmotte, J. Parmentier, A. Celzard, Reaction of condensed tannins with ammonia, Industrial Crops and Products. 44 (2013) 330–335. https://doi.org/10.1016/j.indcrop.2012.11.024.

[131] F.L. Braghiroli, V. Fierro, M.T. Izquierdo, J. Parmentier, A. Pizzi, A. Celzard, Nitrogen-doped carbon materials produced from hydrothermally treated tannin, Carbon. 50 (2012) 5411–5420. https://doi.org/10.1016/j.carbon.2012.07.027.

[132] F.L. Braghiroli, V. Fierro, A. Szczurek, N. Stein, J. Parmentier, A. Celzard, Hydrothermally treated aminated tannin as precursor of N-doped carbon gels for supercapacitors, Carbon. 90 (2015) 63–74. https://doi.org/10.1016/j.carbon.2015.03.038.

[133] F.L. Braghiroli, V. Fierro, A. Szczurek, N. Stein, J. Parmentier, A. Celzard, Electrochemical performances of hydrothermal tannin-based carbons doped with nitrogen, Industrial Crops and Products. 70 (2015) 332–340. https://doi.org/10.1016/j.indcrop.2015.03.046.

[134] F.L. Braghiroli, V. Fierro, M.T. Izquierdo, J. Parmentier, A. Pizzi, A. Celzard, Kinetics of the hydrothermal treatment of tannin for producing carbonaceous microspheres, Bioresource Technology. 151 (2014) 271–277. https://doi.org/10.1016/j.biortech.2013.10.045.

[135] F.L. Braghiroli, V. Fierro, J. Parmentier, L. Vidal, P. Gadonneix, A. Celzard, Hydrothermal carbons produced from tannin by modification of the reaction medium: Addition of H+ and Ag+, Industrial Crops and Products. 77 (2015) 364–374. https://doi.org/10.1016/j.indcrop.2015.09.010.

[136] F.L. Braghiroli, V. Fierro, A. Szczurek, P. Gadonneix, J. Ghanbaja, J. Parmentier, G. Medjahdi, A. Celzard, Hydrothermal treatment of tannin: A route to porous metal oxides and metal/carbon hybrid materials, Inorganics. 5 (2017) 7. https://doi.org/10.3390/inorganics5010007.

[137] F.L. Braghiroli, V. Fierro, M.T. Izquierdo, J. Parmentier, A. Pizzi, L. Delmotte, P. Fioux, A. Celzard, High surface – highly N-doped carbons from hydrothermally treated tannin, Industrial Crops and Products. 66 (2015) 282–290. https://doi.org/10.1016/j.ijhydene.2013.06.048.

[138] S. Schaefer, A. Ramirez, R. Mallada, M.T. Izquierdo, J. Santamaria, A. Celzard, V. Fierro, Easy preparation of tannin-based Ag catalysts for ethylene epoxidation, ChemistrySelect. 2 (2017) 8509–8516. https://doi.org/10.1002/slct.201701548.

[139] K. Jurkiewicz, Ł. Hawełek, K. Balin, J. Szade, F.L. Braghiroli, V. Fierro, A. Celzard, A. Burian, Conversion of Natural Tannin to Hydrothermal and Graphene-Like Carbons Studied by Wide-Angle X-ray Scattering, J. Phys. Chem. A. 119 (2015) 8692–8701. https://doi.org/10.1021/acs.jpca.5b02407.